

3 Reverse Engineering Swarm Behaviors Through Turing Learning

As mentioned in Chapter 1, swarm behaviors are emergent behaviors that arise from the interactions of a number of simple individuals in a group [17]. To understand swarm behaviors, researchers in artificial intelligence and swarm robotics use simulated agents or physical robots to mimic the swarm behaviors such as foraging, aggregation and flocking observed in nature. This approach is what we refer to as understanding from synthesis, and it has been shown to provide a deep insight to validate the models of swarm behaviors or generate new hypothesis [140]. The design of the controllers for the agents and robots comply with some common principles. For example, the controllers are distributed, that is, there is no central control for the swarm. The structure of the controllers is relatively simple.

In this chapter, we demonstrate how the proposed system identification (coevolutionary) method allows a machine to infer the behavioral rules of a group of homogeneous agents in an autonomous manner. A replica, which resembles the agents under investigation in terms of behavioral capabilities, is mixed into the group. The coevolutionary algorithm consists of two competitive populations: one of *models*, to be executed on the replica, and the other of *classifiers*. The classifiers observe the motion of an individual¹ in the swarm for a fixed time interval. They are not, however, provided with the individual's sensory information. Based on the individual's motion data, a classifier outputs a Boolean value indicating whether the individual is believed to be an agent or replica. The classifier gets a reward if and only if it makes the correct judgment. The fitness of the classifiers thus depends solely on their ability to discriminate between the agents and the replica. Conversely, the fitness of the models depends solely on their ability to 'trick' the classifiers into categorizing them as an agent. Consequently, our method does not rely on

¹Note that 'individual/robot' in the context of swarm behaviors refers to a single unit. It could refer to an agent under investigation or the replica executing a model. However, in the context of evolutionary algorithms (see Section 3.1.1.3), 'individual' refers to a chromosome.

3 Reverse Engineering Swarm Behaviors Through Turing Learning

predefined metrics for measuring the similarity of behavior between models and agents; rather, the metrics (classifiers) are produced automatically in the learning process. Our method is inspired by the Turing test [149, 150], which machines can pass if behaving indistinguishably from humans. Similarly, the models, which evolve, can pass the tests by the coevolving classifiers if behaving indistinguishably from the agents. We hence call our method *Turing Learning*.

To validate the *Turing Learning* method, we present two case studies on canonical problems in swarm robotics: self-organized aggregation [21] and object clustering [22]. We show that observing individual motion is sufficient to guide the learning of these collective behaviors. In this chapter, we only present the simulation results (a real world validation using physical robots based on one of the case studies will be presented in Chapter 4).

This chapter is organized as follows. Section 3.1 describes the implementation of *Turing Learning* (Section 3.1.1) and the two swarm behaviors (Section 3.1.2) investigated in this chapter. Section 3.2 introduces the simulation platform (Section 3.2.1) and simulation setups (Section 3.2.2) for performing coevolution runs. Section 3.3 presents the results obtained from the two case studies. Section 3.3.1 analyzes the evolved models from the perspective of both local behaviors and global behaviors. Section 3.3.2 investigates the coevolutionary dynamics. Section 3.3.3 systematically investigates the evolution of classifiers, showing how to construct a robust classifier system to potentially detect abnormal behaviors in the swarm. Section 3.3.4 presents the results of only observing a subset of agents in the swarm. Section 3.3.5 presents a study where an aspect of the agents' morphology (their field of view) and brain (controller) are inferred simultaneously. Section 3.3.6 shows the results of inferring other behaviors. Section 3.3.7 presents a noise study. Section 3.4 summarizes the findings in this chapter.

3.1 Methodology

In this section, we present the *Turing Learning* method and two case studies: self-organized aggregation [21] and object clustering [22]. In both case studies, individuals execute simple behavioral rules that lead to meaningful emergent behaviors on a global level.

3.1.1 Turing Learning

Turing Learning uses a coevolutionary algorithm that comprises two populations: one of models, and one of classifiers. These populations coevolve competitively. In the following, we describe the models, classifiers, optimization algorithm, fitness calculation method and termination criterion.

3.1.1.1 Models

We assume that one or more replicas, which have actuation and sensing abilities that are equivalent to those of the agents under investigation, are available. In this thesis, the replica(s) will be mixed into a group of homogeneous agents. They should therefore be perceived by the agents as con-specifics [140].

Models are executed on replicas. The models can be represented explicitly (e.g., parameters) or implicitly (e.g., artificial neural networks).

3.1.1.2 Classifiers

The classifier can be any algorithm that takes a sequence of data about the observed individual as input, and outputs a decision (i.e., whether the observed individual is believed to be an agent or replica).

We represent the classifier as a recurrent Elman neural network [151], which is shown in Figure 3.1. The network has i inputs, h hidden neurons and one output neuron. Each neuron of the hidden and output layers has a bias. The network has a total of $(i+1)h + h^2 + (h+1)$ parameters, which all assume values in \mathbb{R} . The activation function used in the hidden and the output neurons is the logistic sigmoid function, which has the range $(0, 1)$ and is defined as:

$$\text{sig } x = \frac{1}{1 + e^{-x}} \quad \forall x \in \mathbb{R}. \quad (3.1)$$

The classifier makes judgments about all individuals—both agents and replica. It observes each individual over a set period of time (i.e., a trial). The final value of its output neuron, O , is used to make the judgment: the classifier judges the individual to be a replica if $O < 0.5$, and an agent otherwise. The classifier’s memory (value of hidden neurons) is reset after each judgment.

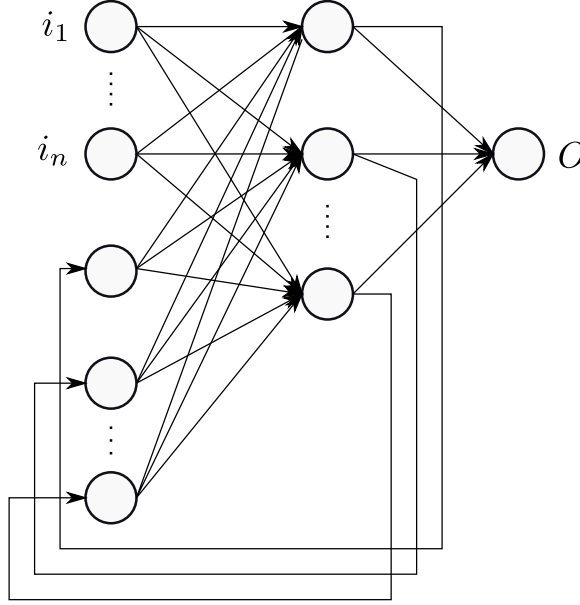


Figure 3.1: The plot shows the structure of a classifier, which is a recurrent Elman neural network, with i inputs, h hidden neurons, and one output neuron (O). O is used for making a judgment. Two bias neurons (which are not shown) with a constant input of 1.0 are connected to each neuron of the hidden and output layers. See text for details.

3.1.1.3 Optimization Algorithm

The optimization of models and classifiers is realized using evolutionary algorithms. In this thesis, we use a $(\mu + \lambda)$ evolution strategy with self-adaptive mutation strengths [152, 153, 154] to optimize either population. The optimization algorithm can be thought of consisting of two sub-algorithms: one for the model population, and another for the classifier population. The sub-algorithms do not interact with each other except for the fitness calculation step (described in Section 3.1.1.4). In each sub-algorithm, the value of μ and λ is equal, which is half of the population size. The implementation of the evolutionary algorithm is detailed as follows.

In this algorithm, an individual is a 2-tuple, $\mathbf{a} = (\mathbf{x}, \boldsymbol{\sigma})$, where $\mathbf{x} \in \mathbb{R}^n$ represents objective parameters, and $\boldsymbol{\sigma} \in (0, \infty)^n$ represents mutation strengths. The i -th mutation strength in $\boldsymbol{\sigma}$ corresponds to the i -th element in \mathbf{x} .

Each generation g comprises a population of μ individuals:

$$\mathcal{P}^{(g)} = \{\mathbf{a}_1^{(g)}, \mathbf{a}_2^{(g)}, \dots, \mathbf{a}_\mu^{(g)}\}.$$

In the population of the first generation, $\mathcal{P}^{(0)}$, all the objective parameters are initialized to 0.0 and all the mutation strengths are initialized to 1.0. Thereafter, in every generation g , the μ parent individuals are first used to create λ offspring individuals by recombination. For the generation of each recombined individual $\mathbf{a}_k'^{(g)}$, $k \in \{1, 2, \dots, \lambda\}$, two individuals are chosen randomly, with replacement, from the parent population: $\mathbf{a}_\chi^{(g)}$ and $\mathbf{a}_\psi^{(g)}$, where $\chi, \psi \in \{1, 2, \dots, \mu\}$. The intermediate population, $\mathcal{P}'^{(g)}$, is produced using discrete and intermediate recombination, which generates the objective parameters and the mutation strengths of the recombined individual, respectively:

$$x_{k,i}'^{(g)} = x_{\chi,i}^{(g)} \quad \text{OR} \quad x_{\psi,i}^{(g)}, \quad (3.2)$$

$$\sigma_{k,i}'^{(g)} = \left(\sigma_{\chi,i}^{(g)} + \sigma_{\psi,i}^{(g)} \right) / 2, \quad (3.3)$$

where $i \in \{1, 2, \dots, n\}$ is indexing the elements within the vectors and, in Equation 3.2, the selection is performed randomly and with equal probability.

Each of the λ recombined individuals is then mutated in order to obtain the final offspring population, $\mathcal{P}''^{(g)}$. This is done according to:

$$\sigma_{k,i}''^{(g)} = \sigma_{k,i}'^{(g)} \exp \left(\tau' \mathcal{N}_k(0, 1) + \tau \mathcal{N}_{k,i}(0, 1) \right), \quad (3.4)$$

$$x_{k,i}''^{(g)} = x_{k,i}'^{(g)} + \sigma_{k,i}''^{(g)} \mathcal{N}_{k,i}(0, 1), \quad (3.5)$$

for all $\{k, i\}$, where $k \in \{1, 2, \dots, \lambda\}$ is indexing the individuals within the population and $i \in \{1, 2, \dots, n\}$ is indexing the elements within the vectors. Equation 3.4 generates the perturbed mutation strength from the original one according to a log-normal distribution. Equation 3.5 mutates the objective parameter according to a normal distribution having the perturbed mutation strength as its deviation. In Equation 3.4, $\mathcal{N}_k(0, 1)$ and $\mathcal{N}_{k,i}(0, 1)$ are both random numbers generated from a standard normal distribution; however, the former is generated once for each individual (i.e. for each value of k), while the latter is generated separately for each element within each individual (i.e. for each combination of k and i). The parameters τ' and τ determine the learning rates of the mutation strengths, and are set as $\tau' = 1/2\sqrt{2n}$, $\tau = 1/2\sqrt{2\sqrt{n}}$ (similar to [155]), where n corresponds to the population size.

Once the offspring population has been generated, the μ individuals with the highest fitness from the combined population, $\mathcal{P}^{(g)} \cup \mathcal{P}''^{(g)}$ (which contains $\mu + \lambda$ individuals), are selected as the parents to form the population of the next generation, $\mathcal{P}^{(g+1)}$. Individuals with an equal fitness have an equal chance of being selected.

3.1.1.4 Fitness Calculation

Let the population sizes for the models and classifiers in the coevolution be M and C , respectively. Let the number of replicas and agents in a trial be n_r and n_a , respectively. n_t trials are conducted for a model in each generation; throughout this thesis, we assume $n_t = 1$.

In our thesis, whenever multiple replicas are used, each of them executes a different model. The fitness of each model in a trial is determined by each of the C classifiers in the competing population. For every classifier that wrongly judges the model as an agent, the model's fitness increases by 1. After all evaluations, the model's fitness takes a value in $\{0, 1, 2, \dots, C\}$. This value is then normalized to $[0, 1]$.

The fitness of each classifier in a trial is determined by its judgments for the n_r replicas (each executing a different model) and n_a agents. For each correct judgment of the replica, the classifier's fitness increases by $\frac{1}{2n_r}$; for each correct judgment of the agent, the classifier's fitness increases by $\frac{1}{2n_a}$. Therefore, the fitness of each classifier in a trial is in range $[0, 1]$. $\left\lceil \frac{M}{n_r} \right\rceil$ trials² are conducted in each generation, and the fitness value of each classifier is then normalized to $[0, 1]$.

3.1.1.5 Termination Criterion

The coevolutionary algorithm stops after running for a fixed number of generations.

3.1.2 Case Studies

3.1.2.1 Problem Formulation

The agents used in our case studies are embodied and move in a two-dimensional, continuous space. The agents' embodiment is based on the e-puck [156], which is a miniature,

²We suggest choosing n_r to be a factor of M .

differential-wheeled robot. Figure 3.2 shows an e-puck robot used in the physical experiments in Chapter 4.

Each agent is equipped with a line-of-sight sensor that it can use to detect the item (e.g., the background, other agents or objects [21], [22]) in front of it.

The swarm behaviors investigated in this thesis use a reactive control architecture, as found in many biological systems³. The motion of each agent solely depends on the state of its line-of-sight sensor (I). Each possible sensor state, $I \in \{0, 1, \dots, n-1\}$, is mapped onto a pair of predefined velocities for the left and right wheels, $(v_{\ell I}, v_{r I})$. $v_{\ell I}, v_{r I} \in [-1, 1]$ represent the normalized left and right wheel velocities, respectively, where 1 (−1) corresponds to the wheel rotating forwards (backwards) with maximum velocity. Given n sensor states, any reactive behavior can thus be represented using $2n$ system parameters. In the remainder of this thesis, we describe the corresponding controllers by writing the $2n$ parameters as a tuple in the following order:

$$\mathbf{p} = (v_{\ell 0}, v_{r 0}, v_{\ell 1}, v_{r 1}, \dots, v_{\ell(n-1)}, v_{r(n-1)}). \quad (3.6)$$

We assume that the replica has the same differential drive and line-of-sight sensor⁴ as the agents. The system identification task is thus to infer the control parameters in Equation (3.6). This explicit representation makes it possible for us to objectively measure the quality of the obtained models in the post-evaluation analysis (as discussed in the results section). To make the evolution more challenging, the search space for the algorithm in simulation is unbounded. That is, the model parameters are unconstrained, and the replica can move with arbitrary speed.

The classifier does not have any prior knowledge about the individual under investigation. It is fed with the sequence of motion data of the individual. It has two input neurons ($i = 2$), five hidden neurons ($h = 5$) and one output neuron. The input neurons represent the linear speed (v) and angular speed (ω) of the individual. They are obtained by tracking the positions and orientations of individuals. In simulation, the tracking is noise-free (situations with noise being present are considered in Section 3.3.7 and the physical experiments in Chapter 4 where noise is inherently present). We define the

³For example, researchers have found that the complex auditory orientation behavior of female crickets is derived from simple reactive motor responses to specific sound pulses [95].

⁴In Section 3.3.5, we show that this assumption can be relaxed by also evolving some aspect of the agent's morphology.

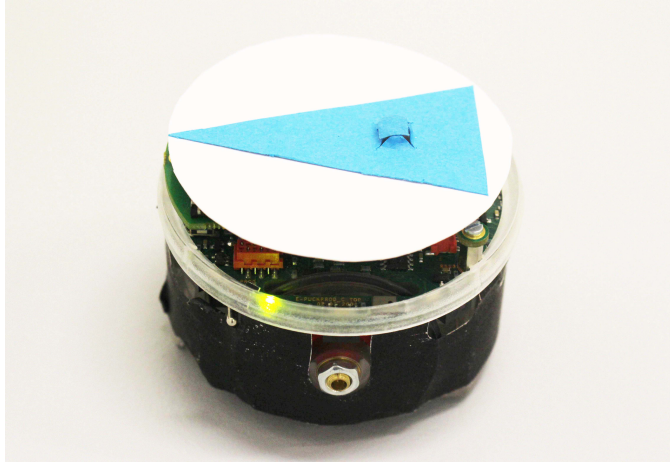


Figure 3.2: An e-puck robot fitted with a black ‘skirt’ and a top marker for motion tracking.

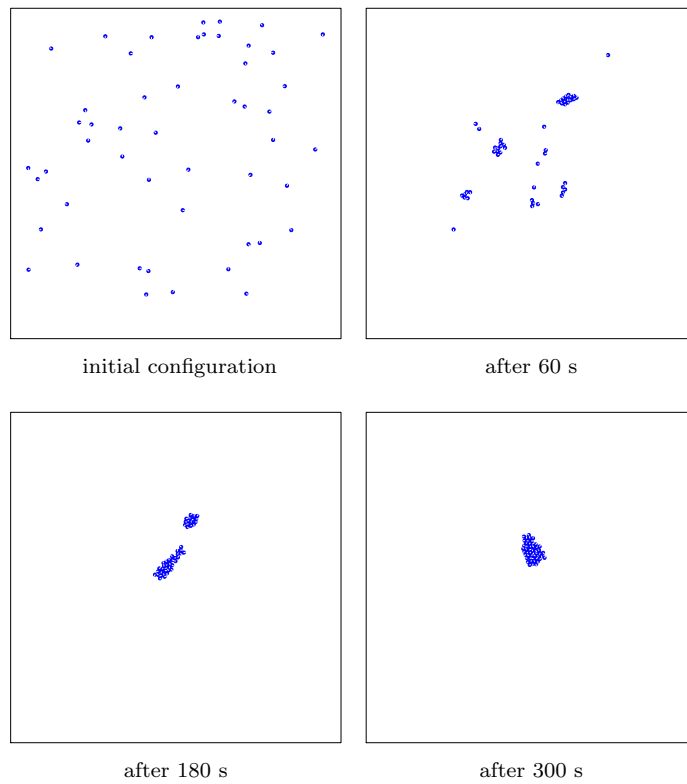


Figure 3.3: Snapshots of the aggregation behavior of 50 agents in simulation.

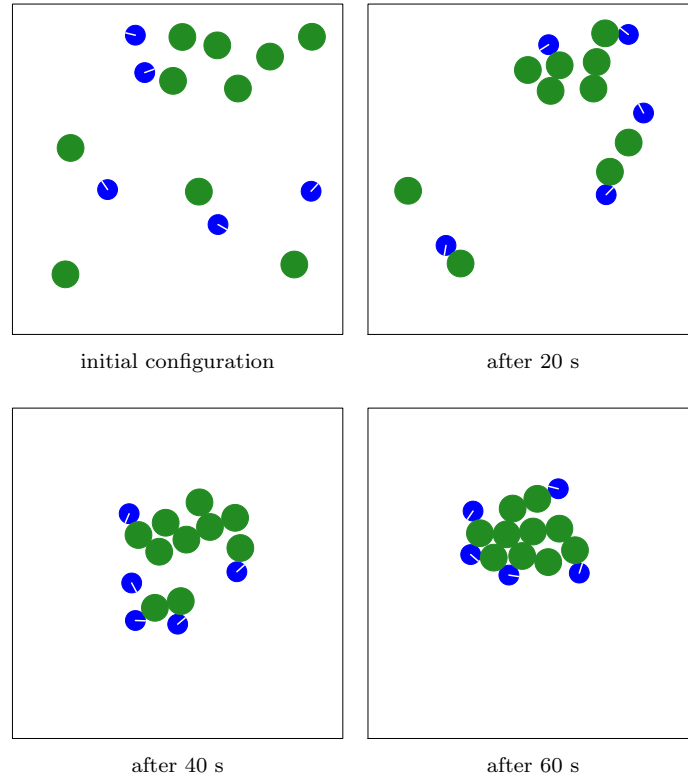


Figure 3.4: Snapshots of the object clustering behavior in simulation. There are 5 agents (blue) and 10 objects (green).

linear speed to be positive when the angle between the individual's orientation and its direction of motion is smaller than $\pi/2$ rad, and negative otherwise.

In the following, we detail the behavioral rules of the two swarm behaviors.

3.1.2.2 Aggregation

In this behavior, the sensor is binary, that is, $n = 2$. It gives a reading of $I = 1$ if there is an agent in the line of sight, and $I = 0$ otherwise. The environment is free of obstacles. The objective for the agents is to aggregate into a single compact cluster as fast as possible. Further details, including a validation with 40 physical e-puck robots, are reported in [21].

The 'optimal' controller for aggregation was found by performing a grid search over the entire space of possible controllers (with finite resolution) [21]. The 'optimal' controller's

parameters are:

$$\mathbf{p} = (-0.7, -1.0, 1.0, -1.0). \quad (3.7)$$

When $I = 0$, an agent moves backwards along a clockwise circular trajectory ($v_{\ell 0} = -0.7$ and $v_{r0} = -1.0$). When $I = 1$, an agent rotates clockwise on the spot with maximum angular velocity ($v_{\ell 1} = 1.0$ and $v_{r1} = -1.0$). Note that rather counter-intuitively, an agent never moves forward, regardless of I . With this controller, an agent provably aggregates with another agent or a quasi-static cluster of agents [21]. Figure 3.3 shows snapshots from a simulation trial with 50 agents.

3.1.2.3 Object Clustering

This behavior uses $n = 3$ sensor states: $I = 0$ if the sensor is pointing at the background (e.g., the wall of the environment, if the latter is bounded), $I = 1$ if the sensor is pointing at an object, and $I = 2$ if it is pointing at another agent. The objective of the agents is to arrange the objects into a single compact cluster as fast as possible. Details of this behavior, including a validation using 5 physical e-puck robots and 20 cylindrical objects, are presented in [22].

The controller's parameters, found using an evolutionary algorithm [22], are:

$$\mathbf{p} = (0.5, 1.0, 1.0, 0.5, 0.1, 0.5). \quad (3.8)$$

When $I = 0$ and $I = 2$, the agent moves forward along an anti-clockwise circular trajectory, but with different linear and angular speeds. When $I = 1$, it moves forward along a clockwise circular trajectory. Figure 3.4 shows snapshots from a simulation trial with 5 agents and 10 objects.

3.2 Simulation Platform and Setups

In this section, we present the agent platform for simulating the two swarm behaviors under investigation and the simulation setups for performing coevolution runs.

3.2.1 Simulation Platform

We use the open-source Enki library [158], which models the kinematics and dynamics of rigid objects, and handles collisions. Enki has a built-in 2-D model of the e-puck. The robot is represented as a disk of diameter 7.0 cm and mass 150 g. The inter-wheel distance is 5.1 cm. The speed of each wheel can be set independently. Enki induces noise on each wheel speed by multiplying the set value by a number in the range (0.95, 1.05) chosen randomly with uniform distribution. The maximum speed of the e-puck is 12.8 cm/s, forward or backward. The line-of-sight sensor is simulated by casting a ray from the e-puck’s front and checking the first item with which it intersects (if any). The range of this sensor is unlimited in simulation.

In the object clustering case study, we model objects as disks of diameter 10 cm with mass 35 g and a coefficient of static friction with the ground of 0.58, which makes it movable by a single e-puck.

The robot’s control cycle is updated every 0.1 s, and the physics is updated every 0.01 s.

3.2.2 Simulation Setups

In all simulations, we used an unbounded environment. For the aggregation case study, we used groups of 11 individuals—10 agents and 1 replica that executes a model. The initial positions of individuals were generated randomly in a square region of sides 331.66 cm, following a uniform distribution (average area per individual = 10000 cm²). For the object clustering case study, we used groups of 5 individuals—4 agents and 1 replica that executes a model—and 10 cylindrical objects. The initial positions of individuals and objects were generated randomly in a square region of sides 100 cm, following a uniform distribution (average area per object = 1000 cm²). In both case studies, individual starting orientations were chosen randomly in $[-\pi, \pi]$ with uniform distribution.

We performed 30 coevolution runs for each case study. Each run lasted 1000 generations. The model and classifier populations each consisted of 100 solutions ($\mu = 50$, $\lambda = 50$). In each trial, classifiers observed individuals for 10 s at 0.1 s intervals (100 data points).

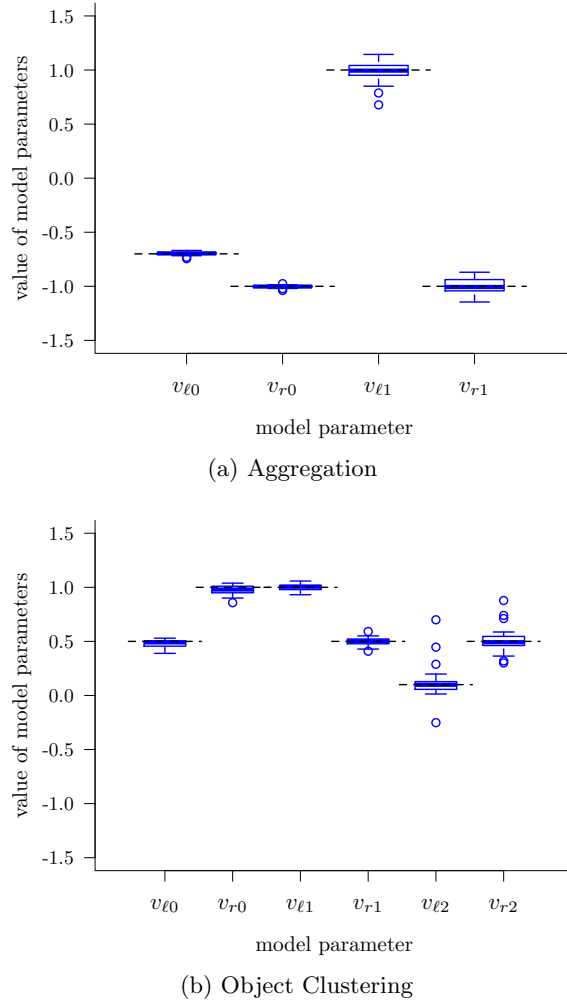


Figure 3.5: Parameters of the evolved models with the highest subjective fitness in the 1000th generation in the coevolutions for (a) the aggregation behavior and (b) the object clustering behavior. Each box corresponds to 30 coevolution runs in simulation. The dotted black lines correspond to the values of the parameters that the system is expected to learn (i.e., those of the agent).

3.3 Simulation Results

3.3.1 Analysis of Evolved Models

In order to objectively measure the quality of the models obtained through *Turing Learning*, we define two metrics. Given an evolved controller (model) \mathbf{x} and the original agent

controller \mathbf{p} , where $\mathbf{x}, \mathbf{p} \in [-1, 1]^{2n}$, we define the absolute error (AE) in a particular parameter $i \in \{1, 2, \dots, 2n\}$ as:

$$\text{AE}_i = |x_i - p_i|. \quad (3.9)$$

We define the mean absolute error (MAE) over all parameters as:

$$\text{MAE} = \frac{1}{2n} \sum_{i=1}^{2n} \text{AE}_i. \quad (3.10)$$

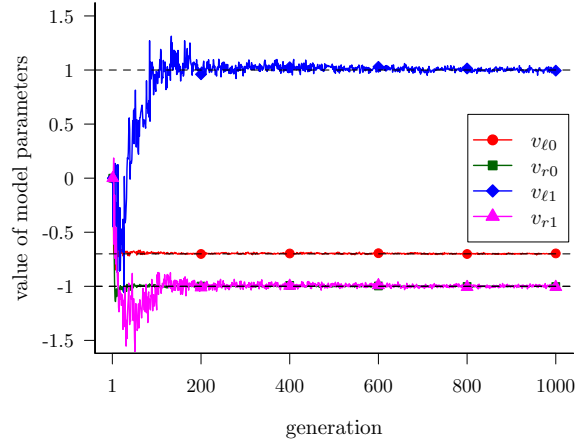
Fig. 3.5 shows a box plot⁵ with the parameters of the evolved models with the highest subjective fitness⁶ in the final generation. It can be seen that *Turing Learning* identified the parameters for both behaviors with good accuracy (dotted black lines represent the ground truth, that is, the parameters of the observed swarming agents). In the case of aggregation, the means (standard deviations) of the AEs in the parameters were (from left to right in Fig. 3.5(a)): 0.01 (0.01), 0.01 (0.01), 0.07 (0.07) and 0.06 (0.04). In the case of object clustering, these values were: 0.03 (0.03), 0.04 (0.03), 0.02 (0.02), 0.03 (0.03), 0.08 (0.13) and 0.08 (0.09).

We also investigated the evolutionary dynamics. Fig. 3.6 shows how the model parameters converged over generations. In the aggregation case study, the parameters corresponding to $I = 0$ were learned first. After around 50 generations, both $v_{\ell 0}$ and $v_{r 0}$ closely approximated their true values (-0.7 and -1.0), shown in Fig. 3.6(a). For $I = 1$, it took about 200 generations for both $v_{\ell 1}$ and $v_{r 1}$ to converge. A likely reason for this effect is that an agent spends a larger proportion of its time seeing nothing ($I = 0$) than other agents ($I = 1$)—simulations revealed these percentages to be 91.2% and 8.8%, respectively (mean values across 100 trials).

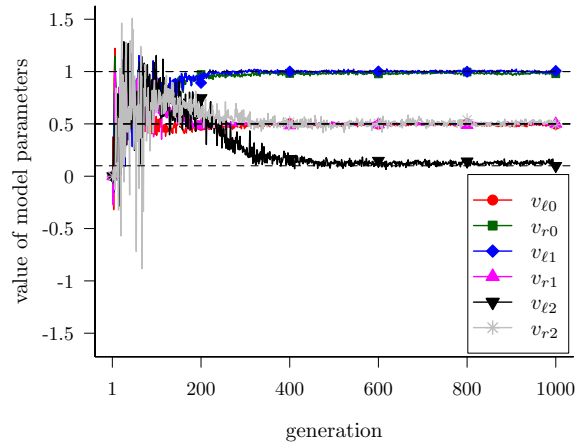
In the object clustering case study, the parameters corresponding to $I = 0$ and $I = 1$ were learned faster than the parameters corresponding to $I = 2$, as shown in Fig. 3.6(b). After about 200 generations, $v_{\ell 0}$, $v_{r 0}$, $v_{\ell 1}$ and $v_{r 1}$ started to converge; however it took about 400 generations for $v_{\ell 2}$ and $v_{r 2}$ to approximate their true values. Note that an

⁵The box plots presented here are all as follows. The line inside the box represents the median of the data. The edges of the box represent the lower and the upper quartiles of the data, whereas the whiskers represent the lowest and the highest data points that are within 1.5 times the range from the lower and the upper quartiles, respectively. Circles represent outliers.

⁶The fitness of the models depends solely on the judgments of the classifiers from the competing population, and is hence referred to as *subjective*.



(a) Aggregation

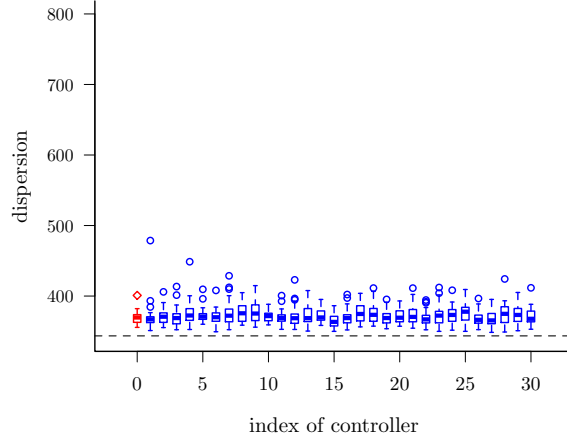


(b) Object Clustering

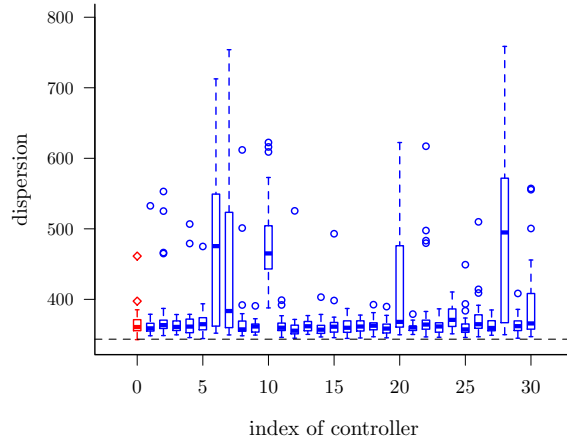
Figure 3.6: Evolutionary process of the evolved model parameters for (a) the aggregation behavior and (b) the object clustering behavior. Curves represent median values across 30 coevolution runs. Dotted black lines indicate true values.

agent spends the highest proportion of its time seeing nothing ($I = 0$), followed by objects ($I = 1$) and other agents ($I = 2$)—simulations revealed these proportions to be 53.2%, 34.2% and 12.6%, respectively (mean values across 100 trials).

Although the evolved models approximate the agents well in terms of parameters, it has often been observed in swarm systems that small changes in individual agent behaviors can lead to vastly different emergent behaviors, especially with large numbers of agents [160]. For this reason, we evaluated the quality of the emergent behaviors that the models give rise to. In the case of aggregation, a good measure of the emergent behavior



(a) Aggregation



(b) Object Clustering

Figure 3.7: (a) Dispersion (after 400 s) of 50 agents executing the original aggregation controller (red box) or one of the 30 evolved models (blue boxes) of the 1000th generation. (b) Dispersion (after 400 s) of 50 objects in a swarm of 25 agents executing the original object clustering controller (red box) or one of the 30 evolved models (blue boxes). In both (a) and (b), boxes show distributions over 30 trials. The dotted black lines indicate the minimum dispersion that 50 agents/objects can possible achieve [159]. See Section 3.3.1 for details.

is the dispersion of the swarm after some elapsed time as defined in [21]⁷. For each of the 30 models with the highest subjective fitness in the final generation, we performed 30 trials with 50 agents each executing the model. For comparison, we also performed 30 trials using the original controller (see Equation (3.7)). The set of initial configurations

⁷The measure of dispersion is based on the robots’/objects’ distances from their centroid. For a formal definition, see Equation (5) of [21], Equation (2) of [22] and [159].

was the same for all models and the original controller. Fig 3.7(a) shows the dispersion for the original controller and models after 400s. All models led to aggregation. We performed a statistical test⁸ on the final dispersion of the agents between the original controller and each model. There was no statistically significant difference in 26 out of 30 cases (30 out of 30 cases with Bonferroni correction).

In the case of object clustering, we use the dispersion of the objects after some elapsed time as a measure of the emergent behavior. With the original controller (see Equation (3.8)) and each of the models, we performed 30 trials with 25 agents and 50 objects. The results are shown in Fig. 3.7(b). In a statistical test on the final dispersion of the objects between the original controller and each model, there was no statistically significant difference in 24 out of 30 cases (26 out of 30 cases with Bonferroni correction).

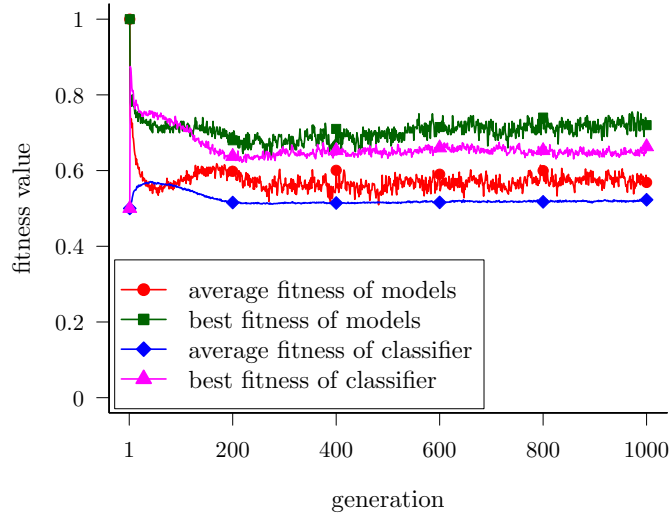
We also investigated the evolutionary process of the model parameters. Figure 3.6 shows the convergence of the model parameters over generations. In the aggregation behavior, the parameters corresponding to $I = 0$ were learned first. After about 50 generations, both $v_{\ell 0}$ and $v_{r 0}$ closely approximated their true values (-0.7 and -1.0) shown in Figure 3.5(a). For $I = 1$, it took about 200 generations for both $v_{l 1}$ and $v_{r 1}$ to converge. A likely reason for this effect is that an agent spends a larger percentage of its time seeing nothing ($I = 0$) than other agents ($I = 1$)—simulations revealed these percentages to be 8.8% and 91.2%, respectively (mean values over 100 trials).

In the object clustering behavior, the parameters corresponding to $I = 0$ and $I = 1$ were learned faster than the other two parameters corresponding to $I = 2$, as shown in the Figure 3.6(b). After about 200 generations, $v_{\ell 0}$, $v_{r 0}$, $v_{l 1}$ and $v_{r 1}$ started to converge; however it took about 400 generations for $v_{l 2}$ and $v_{r 2}$ to approximate their true values. This is likely because an agent spends the most percentage of its time seeing nothing ($I = 0$), followed by objects ($I = 1$) and other agents ($I = 2$)—simulations revealed these percentages to be 53.2%, 34.2% and 12.6% , respectively (mean values over 100 trials).

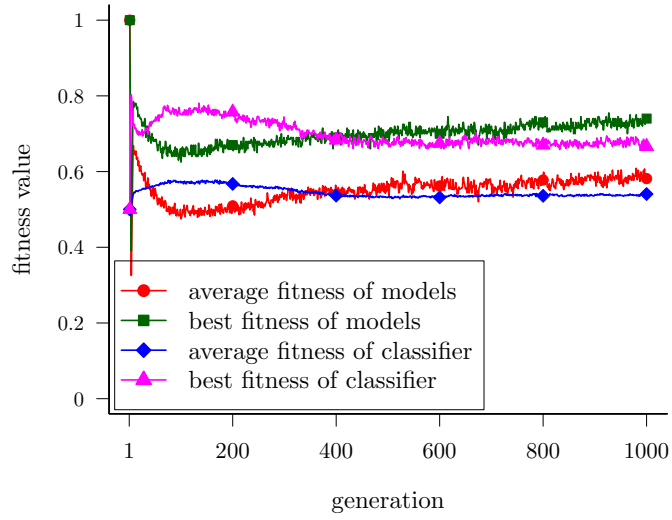
3.3.2 Coevolutionary Dynamics

In order to analyze how the classifiers and the models interact with each other during the course of the coevolution, we investigate the dynamics of the subjective fitness of

⁸Throughout this paper, the statistical test used is a two-sided Mann-Whitney test with a 5% significance level.



(a) Aggregation



(b) Object Clustering

Figure 3.8: This plot shows the subjective fitness of the classifiers and the models for (a) the aggregation behavior and (b) the object clustering behavior. The curves show the median value across 30 coevolution runs.

the classifiers and the models as shown in Figure 3.8.

In the aggregation behavior, at the beginning, the fitness of the classifiers is 0.5 as they output 1 for all the agents and models, which means the classifiers make uninformed decisions⁹. Therefore, the fitness of the models starts from 1.0, as all the classifiers

⁹Note that in the implementation of the coevolutionary algorithm, the parameters of the models and

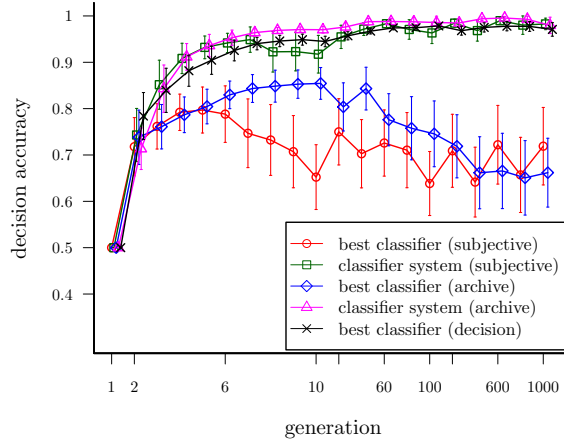


Figure 3.9: The average decision accuracy of the best classifiers and classifier systems over generations (nonlinear scale) in 30 coevolution runs. The error bars show standard deviations. See text for details.

judge them the agent. Then, the average fitness of the classifiers quickly increases, corresponding to the decline of the average fitness of the models. As the models learn to adapt, the average fitness of the classifiers only increases slightly until about the 50th generation. After that, the average fitness of the models starts to increase. However, the best fitness of the classifiers is still higher than that of the models. The best fitness of the models surpasses that of the classifiers after about the 120th generation; at this point, the fitness of the ‘best’ model (selected by the classifiers) is around 0.7. This means that the ‘best’ model is able to mislead 70% of the classifiers into judging it as the agent. From the 200th generation onwards, the fitness of the classifiers and models remains “balanced” until the last generation.

The coevolutionary dynamics of the object clustering behavior is similar. Compared with the dynamics of the aggregation behavior, it takes more generations for the fitness of the models to surpass that of the classifiers. This could be explained by the higher number of parameters and the higher complexity of the behavior to be evolved in the object clustering behavior.

classifiers are initialized to 0.0, which means all the classifiers are identical at the 1st generation.

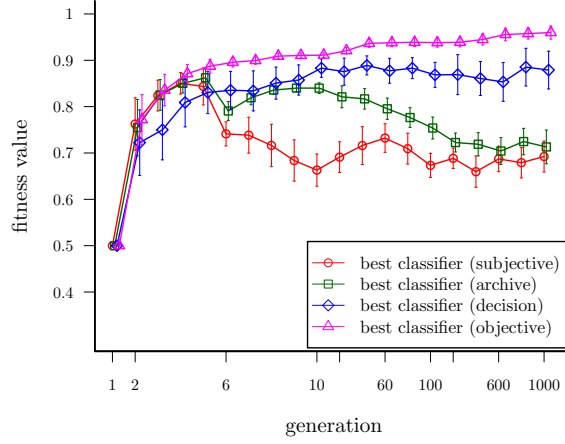


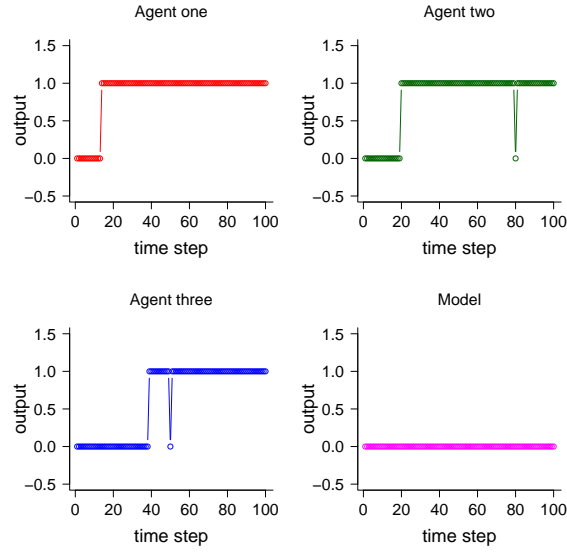
Figure 3.10: This plot shows the average fitness of the classifiers over generations in 30 coevolution runs. The fitness is calculated based on 14641 testing models. See text for details.

3.3.3 Analysis of Evolved Classifiers

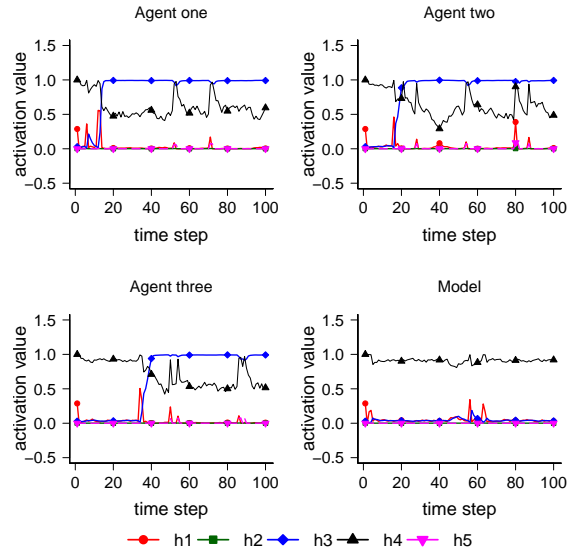
The primary outcome of the *Turing Learning* method (and of any system identification method) is the model, which has been discussed in the previous section. However, the evolved classifiers can also be considered as a useful byproduct. For instance they could be used to detect abnormal agents in a swarm. We will now analyze the performance of the evolved classifiers. For the remainder of this paper, we consider only the aggregation case study.

To assess the performance of the classifiers, we measure the percentage of correct judgments over agents and a wide range of models. The models are uniformly distributed across the entire parameter space of the agents: $[-1, 1]^4$. To keep the analysis of classifiers within a reasonable computation time, we discretize this space using 11 settings per parameter, to obtain: $\mathcal{X} = \{-1.0, -0.8, \dots, 0.8, 1.0\}^4$. This discretized space is a grid consisting of $|\mathcal{X}| = 11^4 = 14641$ points (i.e., models). The classifier’s performance is computed as follows. The model is executed by a replica mixed into a group of 10 agents (as in the coevolution runs). 10 trials are performed using a set of initial configurations common to all classifiers. The motion data is fed to each classifier, which makes 10 judgments per individual. If the classifier consistently judges the individual as a model (i.e. not an agent) in 10 out of 10 trials, it outputs a “model” decision. Otherwise, it outputs “agent”. This conservative approach was used to minimize the risk of false positive detection of abnormal behavior.

3 Reverse Engineering Swarm Behaviors Through Turing Learning



(a) decision-making process



(b) activation of hidden neurons

Figure 3.11: This plot shows the (a) decision-making process and (b) the corresponding activation value of the 5 hidden neurons of a classifier for three random-chosen agents and the replica that executes a very good model in a trial. Hidden neurons are labeled as h1, h2, h3, h4, and h5.

3.3.3.1 Using a Single Classifier

The average decision accuracy of the classifier with the highest subjective fitness in 30 coevolution runs is shown in Fig. 3.9 (*best classifier (subjective)*). The accuracy combines the percentage of correct judgments about models (50% weight) with the percentage of correct judgments about agents (50% weight). The accuracy of the classifier increases in the first 5 generations, then drops and fluctuates within range 62%–80%.

An alternative strategy is to select the classifier that achieves the highest fitness when evaluated on the whole historical tracking data (not just those of the current generation). The decision accuracy of this classifier is also shown in Fig. 3.9 (*best classifier (archive)*). The trend is similar to that of *best classifier (subjective)*. The accuracy increases in the first 10 generations, and then starts *decaying*, dropping to around 65% by the 1000th generation. However, in the earlier generations, the accuracy of the *best classifier (archive)* is higher than that of the *best classifier (subjective)*. For a comparison, we also plot the highest decision accuracy that a single classifier achieves for each generation (*best classifier (decision)*). Interestingly, the accuracy of the *best classifier (decision)*, which is shown in Fig. 3.9 (black curve), increases almost monotonically, reaching a level above 95%. Note that to select the *best classifier (decision)*, one needs to perform additional trials (146410 in this case).

At first sight, it is counter-intuitive that selecting the best classifier according to the historical data still leads to low decision accuracy. This phenomenon, however, can be explained when considering the model population. We have shown in the previous section (see especially Fig. 3.6(a)) that the models converge rapidly at the beginning of the coevolutions. As a result, when classifiers are evaluated in later generations, the trials are likely to include models very similar to each other. Classifiers that become overspecialized to this small set of models (the ones dominating the later generations) have a higher chance of being selected in the post-evaluation. These classifiers may however have a low performance when evaluated across the entire model space.

To investigate whether the decision accuracy is a good measurement of the quality of the classifiers, we plot a figure showing the fitness of the best classifiers corresponding to Figure 3.9. The fitness is calculated based on the 14641 models. In addition, we also plot the classifier with the highest fitness for comparison, which is termed as *best classifier (objective)*. The results are shown in Figure 3.10. As we can see, the trend of fitness curves show good correspondence to that of the decision accuracy in Figure 3.9,

although there is still a small gap between the *best classifier (decision)* and *best classifier (objective)*. This means measuring the quality of classifiers according to decision accuracy is a reasonable choice.

In order to understand how the classifiers make judgment, we analyze the internal processing through monitoring the activation of hidden neurons. Figure 3.11 shows the decision-making process and the corresponding activation value of the 5 hidden neurons of the classifier with the highest subjective fitness in the last generation of a coevolution run for 3 randomly-chosen agents and the replica in a trial. The model executed on the replica has a parameter set of $(-0.7, -1.0, 1.0, -0.9)$, which is very near to that of the agent in Equation (3.7). As we can see in Figure 3.11(a), for the agents, the classifier outputs 0 at the beginning, and then starts to output 1 after certain time steps, which means it needs some time to make the correct judgment. Note that for some time steps after it starts to output 1, it still outputs 0, but this happens only occasionally. For the model, it always outputs 0. This phenomenon can be explained by the activation value of the hidden neurons of the classifier in the following paragraph.

The classifier's activation value of the hidden neurons (labeled as h1, h2, h3, h4, and h5) shown in Figure 3.11(b) reveals its internal processing for the motion of different individuals¹⁰. It seems that the decision-making ("sudden jump" in Figure 3.11(a)) of the classifier is most likely related with the variation of h3 and h4. Take the agents for example, at the beginning, h3 has a very low value (which is almost 0) and then after certain time steps it starts to increase. The variation tendency of h4 is opposite. Every time the classifier's judgment starts to jump from 0 to 1, the value of h3 starts to surpass that of h4. h1, h2 and h5 are almost not activated during the whole period, although sometimes the activation of h2 influences the judgment of the classifier. For instance, there are two peaks at about 50th and 80th time step in h2 for agent two and three, which corresponds to a wrong judgment of the classifier (that is, it outputs 0) at the same point. For the model, all the hidden neurons are almost not activated.

3.3.3.2 Using a Classifier System

The results of the previous section have shown that using a single classifier is not a good solution; although there may be a good classifier in each generation, it may take significant effort (trials with agents) to find it.

¹⁰Note that the activation of hidden neurons may not be the same for all the classifiers due to the symmetry of neural networks, but the dynamics of each hidden neuron is similar.

To address this problem, we propose the use of a classifier system, that is, a number of classifiers working in tandem to judge a given candidate. We choose the best 10 classifiers¹¹. This is either the set of 10 classifiers with the highest subjective fitness in the current generation or the set of classifiers that achieve the highest fitness when evaluated on the whole historical data. If one or more classifiers make a decision about the candidate as a model (i.e. not an agent), the system outputs a “model” decision. Otherwise, it outputs “agent”.

The results of using a classifier system are shown in Fig. 3.9 (green and magenta, respectively). The two systems exhibit significantly improved decision accuracy across all generations. After 1000 generations, each system has a high accuracy of above 95%, on average.

When post-evaluating the performance of classifier systems, we kept the setup the same as the one used in the coevolution runs (i.e., 10 agents and 1 replica in each trial). In practice, the ratio of agents and replicas in a trial could be different. Therefore, we analyzed the scalability of the classifier systems selected in the last generation over 30 coevolution runs with different number of agents in the group. Note that there is always one replica in the group. We have verified that with various number of replicas in the group, similar results are obtained. We tested 14641 different models. Figure 3.12 shows the decision accuracy of the *classifier system (archive)* when changing the number of agents in the group. As we can see, the decision accuracy of the classifier system is not affected by the variation of the number of agents, which shows the robustness of the classifier system.

As we mentioned before, we chose 10 classifiers to form a classifier system to have a reasonable decision accuracy. Here we investigate how the classifier systems perform with various number of classifiers chosen to form a system. The decision accuracy of the *classifier system (archive)* is shown in Figure 3.13¹². It seems that as long as the number of classifiers chosen to form a system is within a certain range, the system could perform well. For example, when the number of selected classifiers is between 10 and 25,

¹¹Note that the number of classifiers chosen to form the system here is not necessarily optimal. There is no guarantee that the individually best few classifiers will form the best *system* when working in tandem. In principle, one could exhaustively search every possible combination of a given number of classifiers from the population. However, this is often infeasible—with our settings of choosing 10 classifiers out of 100, 1.73×10^{13} possibilities exist. We therefore propose the heuristic of choosing the individually best classifiers to form the system, and empirically show that this nevertheless yields good results.

¹²The result of *classifier system (subjective)* is similar.

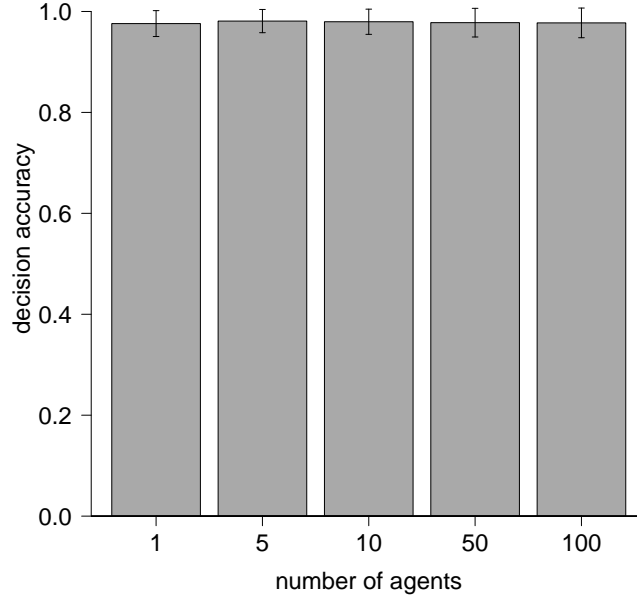


Figure 3.12: This plot shows the decision accuracy of the *classifier system (archive)* in the 1000th generation of 30 coevolution runs for different numbers of agents in the group. In each case, 14641 different models were tested. A single replica was present in each trial.

the classifier system can obtain a high decision accuracy. However, when the number is high (e.g., 75), the decision accuracy declines dramatically.

3.3.4 Observing Only a Subset of Agents

So far, we have used motion data about all agents in the swarm when evaluating classifiers. However, this may not always be feasible in practice. For instance, given a video recording of a large and/or dense swarm, extracting motion data about all agents may be infeasible or lead to highly inaccurate results. A more practical solution might be to only track a subset of agents (e.g., by equipping them with markers).

We now compare the case where all agents are observed with the other extreme, where only one agent is observed. We study how these two cases compare as the swarm size increases. We conducted 30 coevolution runs with each number of agents $n \in \{1, 5, 10, 50, 100\}$. There was always one replica in the group. When observing only one

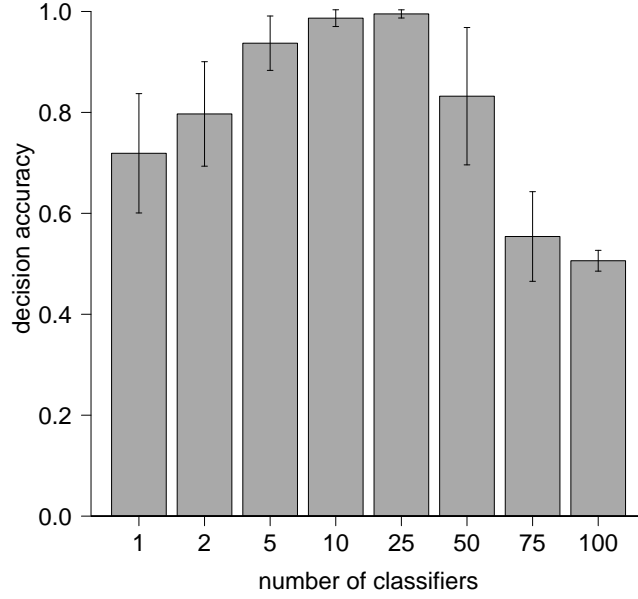


Figure 3.13: This plot shows the decision accuracy of the *classifier system (archive)* in the 1000th generation of 30 coevolution runs with various number of classifiers chosen to form a system.

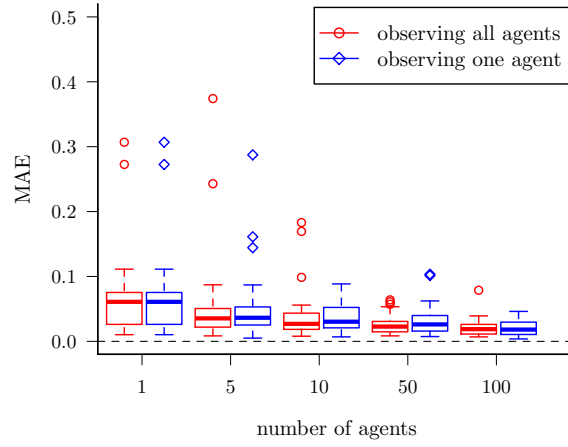


Figure 3.14: MAE (defined in Equation (3.10)) of the evolved models with the highest subjective fitness after 1000 generations, when using *Turing Learning* with varying numbers of agents (excluding the replica). Red and blue boxes show, respectively, the cases where all agents are observed, and one agent is observed. Boxes show distributions over 30 coevolution runs.

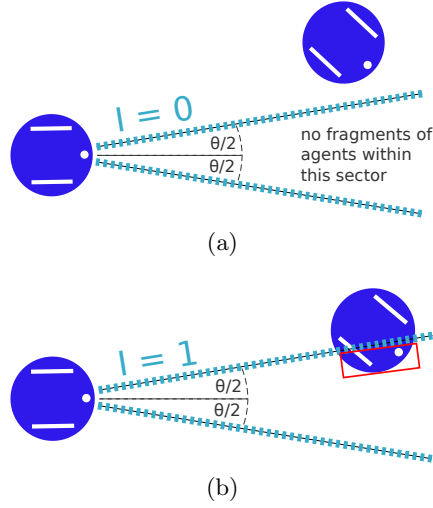


Figure 3.15: A diagram showing the angle of view of the agent's sensor investigated in Section 3.3.5.

agent, this was chosen randomly in each trial. Note that the total number of trials in each coevolution run for the case of observing all agents and one agent is identical. We measured the total square error of the model with the highest subjective fitness in the last (1000th) generation of each run. The results are shown in Fig. 3.14.

There is no statistically significant difference for any n . On the other hand, as the swarm size increases, performance improves. For example, there is a statistically significant difference between $n = 10$ and $n = 100$, both when observing all agents and one. These results suggest that the key factor in the coevolutionary process is not the number of observed agents, so much as the richness of information that comes from increasing inter-agent interactions, and is reflected in each agent's motion. This means that in practice, observing a single agent is sufficient to infer accurate models, as long as the swarm size is sufficiently large.

A similar phenomenon was observed in a different scenario, where the goal was to distinguish between different 'modes' of a swarm (i.e., global behaviors) through observing only a few individuals [161].

3.3.5 Evolving Control and Morphology

In the previous sections, we assumed that we fully knew the agents' morphology (i.e., structure), and only their behavior (controller) was to be identified. We now present a

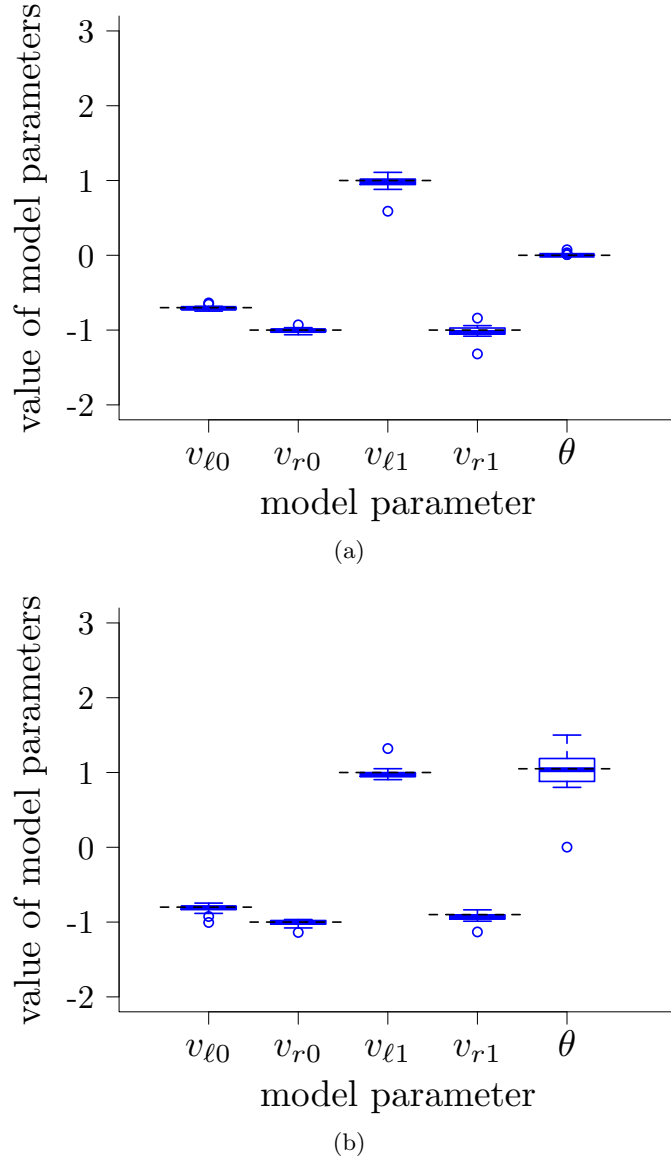


Figure 3.16: Parameters (controller parameters and angle of view in rad) of the evolved models with the highest subjective fitness in the 1000th generation corresponding to the case of the agents' angle of view equal to (a) 0 rad and (b) $\pi/3$ rad. Boxes show distributions over 30 coevolution runs. Dotted black lines indicate true values.

variation where one aspect of the morphology is also unknown. The replica, in addition to the four controller parameters, takes a parameter $\theta \in [0, 2\pi]$ rad, which determines the horizontal field of view of its sensor, as shown in Fig. 3.15 (however, the sensor is still binary). Note that in the previous sections the agents' line-of-sight sensor can be

considered as a sensor with angle of view of 0 rad.

The models now have five parameters. As before, we let the coevolution run in an unbounded search space (i.e., now, \mathbb{R}^5). However, as θ is necessarily bounded, before a model was executed on a replica, the parameter corresponding to θ was mapped to the range $[0, 2\pi]$ using a logistic sigmoid function (Equation (3.1)). The controller parameters were directly passed to the replica. In this setup, the classifiers observed the individuals for 100 s in each trial (preliminary results indicated that this setup requires a longer observation time).

Fig. 3.16(a) shows the parameters of the subjectively best models in the last (1000th) generations of 30 coevolution runs. The means (standard deviations) of the AEs in each model parameter were: 0.02 (0.01), 0.02 (0.02), 0.05 (0.07), 0.06 (0.06) and 0.01 (0.01). All parameters including θ were still learned with high accuracy.

The case where the true value of θ is 0 rad is an edge case, because given an arbitrarily small $\epsilon > 0$, the logistic sigmoid function maps an infinite domain of values onto $(0, \epsilon]$. This makes it easier for the coevolution to learn this parameter. For this reason, we also considered another scenario where the agents' angle of view is $\pi/3$ rad rather than 0 rad. The controller parameters for achieving aggregation in this case are different from those in Equation (3.7). They were found by re-running a grid search with the modified sensor. Fig. 3.16(b) shows the results from 30 coevolutions with this setup. The means (standard deviations) of the AEs in each parameter were: 0.04 (0.04), 0.03 (0.03), 0.05 (0.06), 0.05 (0.05) and 0.20 (0.19). The controller parameters were still learned with good accuracy. The accuracy in the angle of view is noticeably lower, but still reasonable.

3.3.6 Evolving Other Behaviors

The aggregation controller that agents used in our case study was originally synthesized by searching over the space $[-1, 1]^4$, using a metric to assess the swarm's global performance [21]. Other points in this space lead to different global behaviors that can be 'meaningful' to a human observer (e.g. circle formation [112]).

We now investigate whether our coevolutionary method can learn arbitrary controllers in this space, irrespective of the global behaviors they lead to. We generated 1000 controllers randomly in $[-1, 1]^4$, with uniform distribution. For each controller we performed one coevolution run, and selected the subjectively best model in the last (1000th) generation.

Fig. 3.18(a) shows a histogram of the MAE of the evolved models. The distribution has a single mode close to zero, and decays rapidly for increasing values. Over 89% of the 1000 cases have an error below 0.05. This suggests that the accuracy of *Turing Learning* is not highly sensitive to the particular behavior under investigation (i.e., most behaviors are learned equally well). Fig. 3.18(b) shows the AEs of each model parameter. The means (standard deviations) of the AEs in each parameter were: 0.01 (0.05), 0.02 (0.07), 0.07 (0.6) and 0.05 (0.20). We performed a statistical test on the AEs between the model parameters corresponding to $I = 0$ ($v_{\ell 0}$ and $v_{r 0}$) and $I = 1$ ($v_{\ell 1}$ and $v_{r 1}$). The AEs of the evolved $v_{\ell 0}$ and $v_{r 0}$ were significantly lower than those of the evolved $v_{\ell 1}$ and $v_{r 1}$. This was likely due to the reason reported in Section 3.3.1; that is, an agent spends more time seeing nothing ($I = 0$) than other agents ($I = 1$) in each trial.

3.3.7 Noise Study

We conducted a study to investigate how the performance of *Turing Learning* is affected by noise on the measurements of the individuals' position and orientation. As the e-puck robot has a maximum linear speed of 12.8 cm/s, the maximum distance that it can travel in one control cycle (0.1 s) is 1.28 cm. For this reason, we define a disturbance of 1.28 cm to an individual's position as a measurement error of 100%. Similarly, we define a 100% measurement error on the individual's orientation as the maximum change in orientation that an e-puck can undergo in one control cycle. This corresponds to 0.5 rad.

We conducted 5 sets of 30 coevolutions for the noise values $M = \{0, 25, 50, 75, 100\}\%$. In a coevolution with a noise value M , every measurement of an individual's position is perturbed in a random direction and by a random distance chosen uniformly in $[0, 1.28 \frac{M}{100}]$ cm. Similarly, every orientation measurement is perturbed by a random angle chosen uniformly in $[-0.5 \frac{M}{100}, 0.5 \frac{M}{100}]$.

Figure 3.19 shows the total square error of the evolved parameters in the final generations of the coevolutions. This plot reveals that the system still performs relatively well when a considerable amount of noise affects the individuals' motion tracking system.

3.4 Summary

This chapter has presented the simulation results of using the *Turing Learning* method to autonomously learn swarm behaviors through observation. To our knowledge, *Turing*

3 Reverse Engineering Swarm Behaviors Through Turing Learning

Learning is the first system identification method that does not rely on any predefined metric to quantitatively gauge the difference between agents and learned models. This eliminates the need to choose a suitable metric and the bias that such metric may have on the obtained solutions.

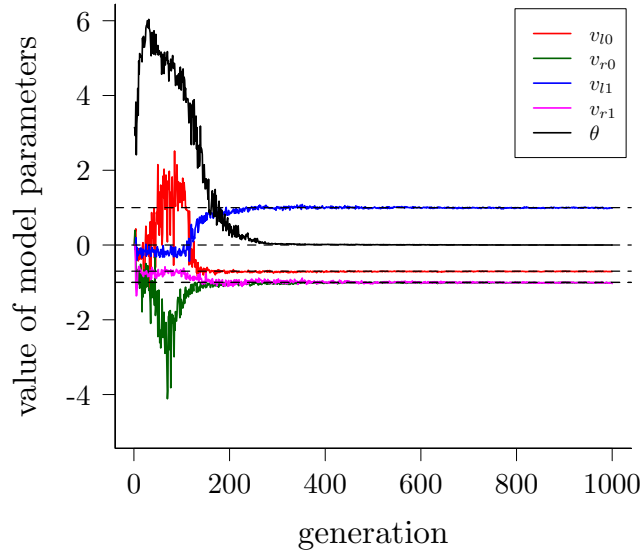
Through competitive coevolution of models and classifiers, the system successfully learned two swarm behaviors (self-organized aggregation and object clustering). Both the model parameters, which were automatically inferred, and emergent global behaviors closely matched those of the original swarm system. We also constructed a robust classifier system that, given an individual's motion data, can tell whether the individual is an original agent or not. Such classifier system could be effective in detecting abnormal behavior, for example, when faults occur in some members of the swarm. Note that *Turing Learning* produces these classifiers automatically without the need to define a priori what constitutes abnormal behavior.

A scalability study showed that the interactions in a swarm can be characterized by the effects on a subset of agents. In other words, when learning swarm behaviors especially with large number of agents, instead of considering the motion of all the agents in the group, we could focus on a subset of agents. This becomes critical when the available data about agents in the swarm is limited. Our approach was proven to work even if using only the motion data of a single agent and replica, as the data from this agent implicitly contained enough information about the interactions in the swarm.

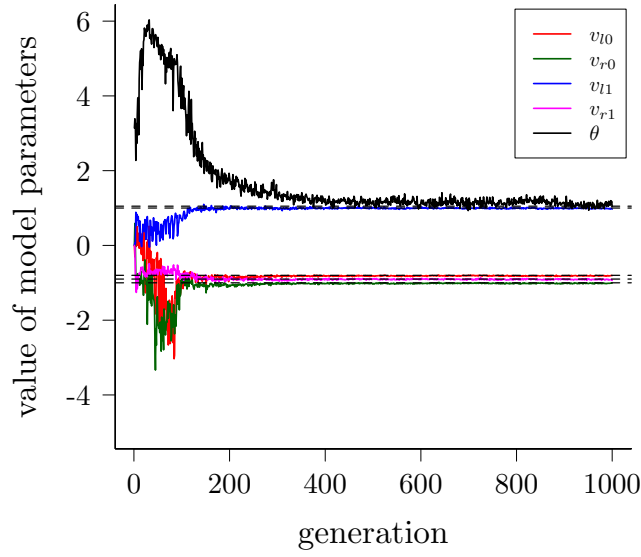
In this thesis, the model was explicitly represented by a set of parameters. The evolved parameters could thus be compared against the ground truth, enabling us to objectively gauge the quality of evolved models in two case studies as well as for 1000 randomly sampled behaviors. In principle, we could also evolve the structure of the agent's control system. The results of learning the agent's angle of view showed that our method may even learn the morphology of the swarming agents.

In collective behavior, abnormal agent(s) may have a great impact on the swarm [110]. For the same reason, the insertion of a replica that exhibits different behavior or is not recognized as con-specific may disrupt the global behavior and hence the models obtained may be biased. An appropriate strategy would be to isolate the influence of the replica. In particular, to evaluate a model one could perform two trials, one with only replicas each executing the model and the other with only agents. The data of the replicas and agents from each trial could then be fed into the classifiers for making judgments. Some

preliminary results suggest that there is no significant difference between either approach for the case studies considered in this paper.

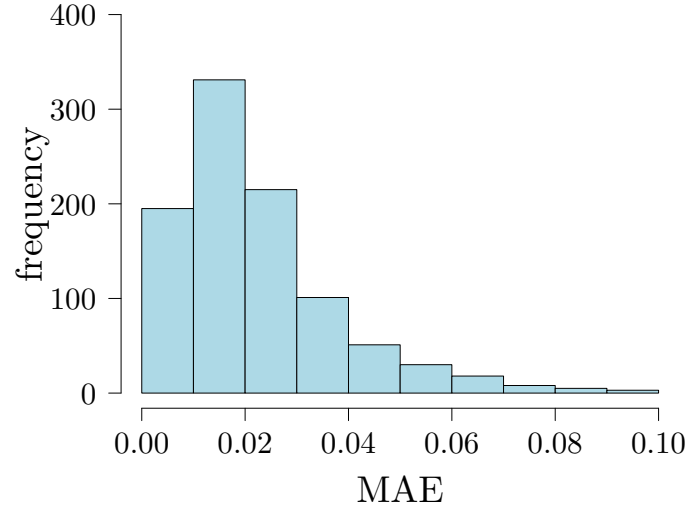


(a)

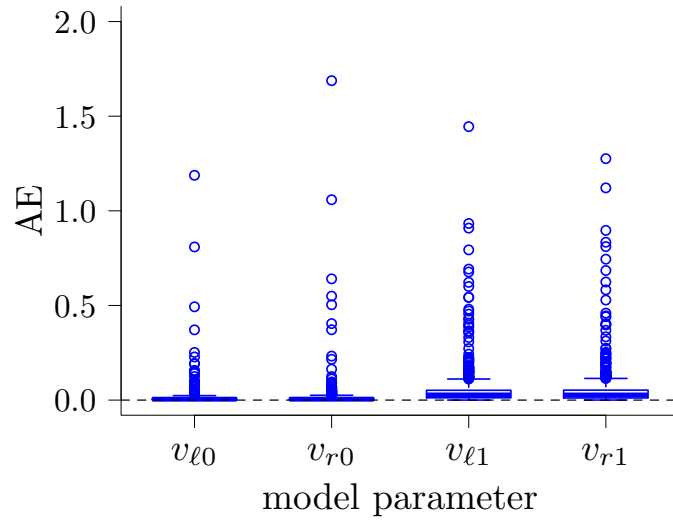


(b)

Figure 3.17: Evolutionary process of the evolved models (controller parameters and angle of view in rad) in the 1000th generation corresponding to the case of the agents' angle of view equal to (a) 0 rad and (b) $\pi/3$ rad. Boxes show distributions over 30 coevolution runs. Dotted black lines indicate true values..



(a)



(b)

Figure 3.18: This plot shows (a) a histogram of the MAE (defined in Equation (3.10)) of the evolved models and (b) the AEs (defined in Equation (3.9)) of each model parameter in the 1000th generation over 1000 random behaviors. For each behavior, we performed one coevolution run. In (a), 43 points that have MAE larger than 0.1 are not shown.

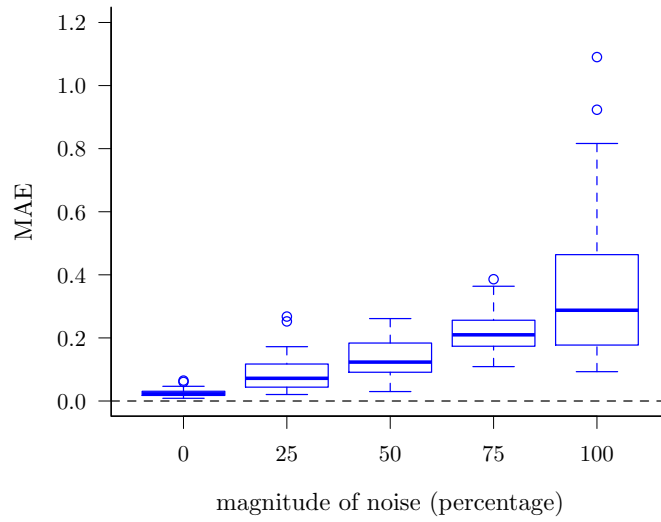


Figure 3.19: This plot shows the total square error of the evolved parameters when increasing the percentage of noise on the measurements of the individuals' position and orientation in the aggregation behavior. Each box corresponds to 30 coevolutionary runs. See text for details.

Bibliography

- [1] J. P. Grotzinger, “Habitability, taphonomy, and the search for organic carbon on mars,” *Science*, vol. 343, no. 6169, pp. 386–387, 2014. [Online]. Available: <http://www.sciencemag.org/content/343/6169/386.short>
- [2] R. P. Hertzberg and A. J. Pope, “High-throughput screening: new technology for the 21st century,” *Current Opinion in Chemical Biology*, vol. 4, no. 4, pp. 445 – 451, 2000. [Online]. Available: <http://www.sciencedirect.com/science/article/pii/S1367593100001101>
- [3] J. Bolhuis and L. Giraldeau, *The behavior of animals: mechanisms, function, and evolution*. USA: Wiley-Blackwell, 2004.
- [4] W. J. Sutherland, “The importance of behavioural studies in conservation biology,” *Animal Behaviour*, vol. 56, no. 4, pp. 801–809, 1998.
- [5] D. Floreano and C. Mattiussi, *Bio-Inspired Artificial Intelligence: Theories, Methods, and Technologies*. Cambridge, MA: MIT Press, 2008.
- [6] J.-A. Meyer and A. Guillot, “Biologically inspired robots,” in *Springer Handbook of Robot.*, ser. Springer Handbooks, B. Siciliano and O. Khatib, Eds. Berlin, Heidelberg, Germany: Springer, 2008, pp. 1395–1422.
- [7] R. King, J. Rowland, S. G. Oliver, and M. Young, “The automation of science,” *Science*, vol. 324, no. 5923, pp. 85–89, 2009. [Online]. Available: <http://www.sciencemag.org/content/324/5923/85.abstract>
- [8] J. Evans and A. Rzhetsky, “Machine science,” *Science*, vol. 329, no. 5990, pp. 399–400, 2010. [Online]. Available: <http://www.sciencemag.org/content/329/5990/399.short>

Bibliography

- [9] D. Waltz and B. G. Buchanan, “Automating science,” *Sci.*, vol. 324, no. 5923, pp. 43–44, 2009.
- [10] L. Ljung, “Perspectives on system identification,” *Annu. Reviews in Control*, vol. 34, no. 1, pp. 1–12, 2010.
- [11] S. A. Billings, *Nonlinear system identification: NARMAX methods in the time, frequency, and spatio-temporal domains*. Hoboken, NJ, USA: Wiley, 2013.
- [12] S. M. Henson and J. L. Hayward, “The mathematics of animal behavior: An interdisciplinary dialogue,” *Notices of the AMS*, vol. 57, no. 10, pp. 1248–1258, 2010.
- [13] E. Bonabeau, “Agent-based modeling: Methods and techniques for simulating human systems,” *PNAS*, vol. 99, no. 10, pp. 7280–7287, 2002.
- [14] J. Bongard and H. Lipson, “Nonlinear system identification using coevolution of models and tests,” *IEEE Trans. Evol. Computation*, vol. 9, no. 4, pp. 361–384, 2005.
- [15] —, “Automated reverse engineering of nonlinear dynamical systems,” *PNAS*, vol. 104, no. 24, pp. 9943–9948, 2007.
- [16] G. D. Ruxton and G. Beauchamp, “The application of genetic algorithms in behavioural ecology, illustrated with a model of anti-predator vigilance,” *Journal of Theoretical Biology*, vol. 250, no. 3, pp. 435–448, 2008.
- [17] S. Camazine, J.-L. Deneubourg, N. R. Franks, *et al.*, *Self-Organization in Biological Systems*. Princeton, NJ: Princeton University Press, 2001.
- [18] D. Helbing and A. Johansson, “Pedestrian, crowd and evacuation dynamics,” in *Extreme Environmental Events*, R. A. Meyers, Ed. Springer, 2011, pp. 697–716.
- [19] J. Harvey, K. Merrick, and H. A. Abbass, “Application of chaos measures to a simplified boids flocking model,” *Swarm Intell.*, vol. 9, no. 1, pp. 23–41, 2015.
- [20] W. S, B. S, F. R, *et al.*, “Modeling collective animal behavior with a cognitive perspective: a methodological framework,” *PLoS ONE*, vol. 7, no. 6, 2012, e38588.

- [21] M. Gauci, J. Chen, W. Li, T. J. Dodd, and R. Groß, “Self-organized aggregation without computation,” *The Int. J. of Robot. Research*, vol. 33, no. 8, pp. 1145–1161, 2014.
- [22] ———, “Clustering objects with robots that do not compute,” in *Proc. 2014 Int. Conf. Autonomous Agents and Multi-Agent Syst.*, IFAAMAS Press, Paris, France, 2014, pp. 421–428.
- [23] H. Schildt, *Artificial intelligence using C*. New York, NY, USA: McGraw-Hill, 1987.
- [24] E. Charniak, *Introduction to artificial intelligence*. Reading, MA, USA: Addison-Wesley, 1985.
- [25] D. B. Fogel, *Evolutionary computation: toward a new philosophy of machine intelligence*. Street Hoboken, NJ, USA: Wiley-IEEE Press, 1995.
- [26] M. L. Minsky, “Logical versus analogical or symbolic versus connectionist or neat versus scruffy,” *AI magazine*, vol. 12, no. 2, pp. 34–51, 1991.
- [27] A. Turing, “Computing machinery and intelligence,” *Mind*, vol. 59, no. 236, pp. 433–460, 1950.
- [28] P. Jackson, *Introduction to expert system*. Boston, MA, USA: Addison-Wesley, 1998.
- [29] M. Newborn, *Kasparov versus Deep Blue: Computer Chess Comes of Age*. New York, NY, USA: Springer-Verlag, 1997.
- [30] L. Zadeh, “Fuzzy sets,” *Information and Control*, vol. 8, pp. 338–353, 1965.
- [31] N. J. Nilsson, “Shakey the robot,” SRI International Technical Note, Tech. Rep., 1984.
- [32] R. Brooks, “A robust layered control system for a mobile robot,” *Robotics and Automation, IEEE Journal of*, vol. 2, no. 1, pp. 14–23, Mar 1986.
- [33] M. Sasaki, T. Kageoka, K. Ogura, H. Kataoka, T. Ueta, and S. Sugihara, “Total laboratory automation in japan: Past, present and the future,” *Clinica Chimica Acta*, vol. 278, no. 2, pp. 217 – 227, 1998. [Online]. Available: <http://www.sciencedirect.com/science/article/pii/S000989819800148X>

Bibliography

- [34] A. Persidis, “High-throughput screening,” *Nature biotechnology*, vol. 16, no. 5, pp. 488–493, 1998.
- [35] K. E. Whelan and R. D. King, “Intelligent software for laboratory automation,” *Trends in Biotechnology*, vol. 22, no. 9, pp. 440–445, 2004.
- [36] N. Gauld and Gaston., “Driving miss daisy: The performance of an automated insect identification system,” *Hymenoptera: evolution, biodiversity and biological-control*, pp. 303–311, 2000.
- [37] N. MacLeod, M. Benfield, and P. Culverhouse, “Time to automate identification,” *Nature*, vol. 467, no. 7312, pp. 154–55, 2010. [Online]. Available: http://www.nature.com/nature/journal/v467/n7312/full/467154a.html?type=access_denied
- [38] C. Darwin, *On the Origin of Species*. England: Dover Publications, 1859.
- [39] J. H. Holland, *Adaptation in Natural and Artificial Systems*. Boston, Massachusetts: MIT Press, 1992.
- [40] M. J. W. Lawrence J. Fogel, Alvin J. Owens, *Artificial Intelligence through Simulated Evolution*. Chichester, UK: Wiley, 1966.
- [41] I. Rechenberg, *Evolutionsstrategie: Optimierung technischer Systeme nach Prinzipien der biologischen Evolution*. Stuttgart: Fromman-Holzboog Verlag, 1994.
- [42] J. Koza, *Genetic Programming*. Cambridge MA: MIT Press, 1992.
- [43] C. Rosin and R. Belew, “New methods for competitive coevolution,” *Evolutionary Computation*, vol. 5, no. 10, pp. 1–29, 1997.
- [44] R. Dawkins and J. R. Krebs, “Arms races between and within species,” *Proceedings of the Royal Society of London. Series B. Biological Sciences*, vol. 205, no. 1161, pp. 489–511, 1979. [Online]. Available: <http://rspb.royalsocietypublishing.org/content/205/1161/489.abstract>
- [45] J. Cartlidge and S. Bullock, “Combating coevolutionary disengagement by reducing parasite virulence,” *Evolutionary Computation*, vol. 12, no. 2, pp. 193–222, 2004.

- [46] P. J. Angeline and J. B. Pollack, “Competitive environments evolve better solutions for complex tasks,” *Bibliometrics*, vol. 155, no. 18, pp. 1–5, 1993.
- [47] L. Panait and S. Luke, “A comparative study of two competitive fitness functions,” in *Proceedings of the Genetic and Evolutionary Computation Conference*. Boston, Massachusetts: MIT Press, 2002, pp. 567–573.
- [48] T. Tan and J. Teo, “Competitive coevolution with k-random opponents for pareto multiobjective optimization,” in *Natural Computation, Third International Conference on*, 2007, pp. 63 – 67. [Online]. Available: <http://citeseerx.ist.psu.edu/viewdoc/summary?doi=?doi=10.1.1.38.3029>
- [49] O. E. David, H. J. van den Herik, M. Koppel, and N. S. Netanyahu, “Genetic algorithms for evolving computer chess programs,” *IEEE Transactions on Evolutionary Computation*, vol. 18, no. 5, pp. 779–789, 2014.
- [50] G. Gutin, A. Yeo, and A. Zverovich, “Traveling salesman should not be greedy: domination analysis of greedy-type heuristics for the {TSP},” *Discrete Applied Mathematics*, vol. 117, no. 13, pp. 81 – 86, 2002. [Online]. Available: <http://www.sciencedirect.com/science/article/pii/S0166218X01001950>
- [51] C. Wang, S. Yu, W. Chen, and C. Sun, “Highly efficient light-trapping structure design inspired by natural evolution,” *Sci. Rep.*, vol. 3, no. 1, pp. 1–7, 2013.
- [52] H. GS, L. JD, and L. DS, “Computer-automated evolution of an x-band antenna for nasa’s space technology 5 mission,” *Evolutionary Computation*, vol. 19, no. 1, pp. 1–23, 2011.
- [53] R. Bellman, *Dynamic Programming and Lagrange Multipliers*. Princeton, NJ, USA: Princeton University Press, 1957.
- [54] J. J. E. Dennis and J. J. Mor, “Quasi-newton methods, motivation and theory,” *SIAM Review*, vol. 19, no. 1, pp. 46–89, 1977.
- [55] J. R. Shewchuk, “An introduction to the conjugate gradient method without the agonizing pain,” Pittsburgh, PA, USA, Tech. Rep., 1994.
- [56] N. Hansen, S. Muller, and P. Koumoutsakos, “Reducing the time complexity of the derandomized evolution strategy with covariance matrix adaptation (cma-es),” *Evolutionary Computation*, vol. 11, no. 1, pp. 1–18, March 2003.

Bibliography

- [57] C. M. Fonseca and P. J. Fleming, “An overview of evolutionary algorithms in multiobjective optimization,” *Evolutionary Computation*, vol. 3, no. 1, pp. 1–16, 1995.
- [58] K. J. R. and J. P. Rice, “Automatic programming of robots using genetic programming,” in *AAAI*. MIT Press, 1992, pp. 1–6.
- [59] R. A. Brooks, “Artificial life and real robots,” in *Proceedings of the First European Conference on Artificial Life*. MIT Press, 1992, pp. 3–10.
- [60] D. Floreano and S. Nolfi, “Adaptive behavior in competing co-evolving species,” in *The 4th European Conference on Artificial Life*. MIT Press, 1997, pp. 378–387.
- [61] D. Floreano, P. Drr, and C. Mattiussi, “Neuroevolution: from architectures to learning,” *Evolutionary Intelligence*, vol. 1, no. 1, pp. 47–62, 2008. [Online]. Available: <http://dx.doi.org/10.1007/s12065-007-0002-4>
- [62] K. O. Stanley and R. Miikkulainen, “Evolving neural networks through augmenting topologies,” *Evolutionary Computation*, vol. 10, no. 2, pp. 99–127, 2002. [Online]. Available: <http://nn.cs.utexas.edu/?stanley:ec02>
- [63] B. D.M. and O. C., “Understanding evolutionary potential in virtual cpu instruction set architectures,” *PLoS ONE*, vol. 8, no. 12, p. e83242, 2013. [Online]. Available: <http://nn.cs.utexas.edu/?stanley:ec02>
- [64] B. Batut, D. P. Parsons, S. Fischer, G. Beslon, and C. Knibbe, “In silico experimental evolution: a tool to test evolutionary scenarios,” in *Proceedings of the Eleventh Annual Research in Computational Molecular Biology (RECOMB) Satellite Workshop on Comparative Genomics*. BioMed Central Ltd, 2013, pp. 1–6.
- [65] J.-M. Montanier and N. Bredeche, “Surviving the Tragedy of Commons: Emergence of Altruism in a Population of Evolving Autonomous Agents,” in *European Conference on Artificial Life*, Paris, France, Aug. 2011. [Online]. Available: <https://hal.inria.fr/inria-00601776>
- [66] W. M, F. D, and K. L, “A quantitative test of hamilton’s rule for the evolution of altruism,” *PLoS Biology*, vol. 9, no. 5, p. e1000615, 2011.
- [67] D. Floreano, S. Mitri, S. Magnenat, and L. Keller, “Evolutionary conditions for the emergence of communication in robots,” *Current Biology*, vol. 17, no. 6,

- pp. 514 – 519, 2007. [Online]. Available: <http://www.sciencedirect.com/science/article/pii/S0960982207009281>
- [68] A. JE and B. JC, “Environmental influence on the evolution of morphological complexity in machines,” *PLoS Computational Biology*, vol. 10, no. 1, p. e1003399, 2014.
 - [69] D. Cliff and G. F. Miller, “Co-evolution of pursuit and evasion ii: Simulation methods and results,” *Proceedings of the Fourth International Conference on Simulation of Adaptive Behavior*, vol. 92, no. 2, pp. 101–106, 1995.
 - [70] D. Floreano, “Evolutionary robotics in behavior engineering and artificial life,” in *Evolutionary Robotics: From Intelligent Robots to Artificial Life. Applied AI Systems, 1998. Evolutionary Robotics Symposium.* AAI Books, 1998.
 - [71] S. Koos, J.-B. Mouret, and S. Doncieux, “The transferability approach: Crossing the reality gap in evolutionary robotics,” *Evolutionary Computation, IEEE Transactions on*, vol. 17, no. 1, pp. 122–145, Feb 2013.
 - [72] S. Koos, A. Cully, and J. Mouret, “Fast damage recovery in robotics with the t-resilience algorithm,” *CoRR*, vol. abs/1302.0386, 2013. [Online]. Available: <http://arxiv.org/abs/1302.0386>
 - [73] D. Floreano and F. Mondada, “Evolution of homing navigation in a real mobile robot,” *IEEE Trans. Syst., Man, and Cybernetics, Part B: Cybernetics*, vol. 26, no. 3, pp. 396–407, 1996.
 - [74] R. Watson, S. Ficie, and J. Pollack, “Embodied evolution: embodying an evolutionary algorithm in a population of robots,” in *Evolutionary Computation, 1999. CEC 99. Proceedings of the 1999 Congress on*, vol. 1, 1999, pp. –342 Vol. 1.
 - [75] A. Eiben, E. Haasdijk, and N. Bredeche, “Embodied, On-line, On-board Evolution for Autonomous Robotics,” in *Symbiotic Multi-Robot Organisms: Reliability, Adaptability, Evolution.*, ser. Series: Cognitive Systems Monographs, S. K. E. P. Levi, Ed. Springer, 2010, vol. 7, pp. 361–382. [Online]. Available: <https://hal.inria.fr/inria-00531455>
 - [76] A. Eiben, S. Kernbach, and E. Haasdijk, “Embodied artificial evolution,” *Evolutionary Intelligence*, vol. 5, no. 4, pp. 261–272, 2012. [Online]. Available: <http://dx.doi.org/10.1007/s12065-012-0071-x>

- [77] A. E. Eiben and J. Smith, “From evolutionary computation to the evolution of things,” *Nature*, vol. 521, no. 7553, pp. 467–482, 2015.
- [78] J. R. Tumbleston, D. Shirvanyants, N. Ermoshkin, R. Januszewicz, A. R. Johnson, D. Kelly, K. Chen, R. Pinschmidt, J. P. Rolland, A. Ermoshkin, E. T. Samulski, and J. M. DeSimone, “Continuous liquid interface production of 3d objects,” *Science*, vol. 347, no. 6228, pp. 1349–1352, 2015. [Online]. Available: <http://www.sciencemag.org/content/347/6228/1349.abstract>
- [79] L. Ljung, “System identification: Theory for the user,” *Englewood Cliffs, NJ: Prentice-Hall*, 1999.
- [80] D. B. Fogel, *System identification through simulated evolution: a machine learning approach to modeling*. Needham, MA, USA: Ginn Press, 1991.
- [81] E. J. Vladislavleva, G. F. Smits, and D. Den Hertog, “Order of nonlinearity as a complexity measure for models generated by symbolic regression via pareto genetic programming,” *Trans. Evol. Comp.*, vol. 13, no. 2, pp. 333–349, Apr. 2009. [Online]. Available: <http://dx.doi.org/10.1109/TEVC.2008.926486>
- [82] J. Bongard and H. Lipson, “Nonlinear system identification using coevolution of models and tests,” *IEEE Trans. Evol. Comput.*, vol. 9, no. 4, pp. 361–384, 2005.
- [83] —, “Automated damage diagnosis and recovery for remote robotics,” in *Proc. 2004 IEEE Int. Conf. Robot. and Autom.*. IEEE Computer Society Press, New Orleans, LA, 2004, pp. 3545–3550.
- [84] —, “Automated robot function recovery after unanticipated failure or environmental change using a minimum of hardware trials,” in *Proc. 2004 NASA/DoD Conf. Evolvable Hardware*. IEEE Computer Society Press, Los Alamitos, CA, 2004, pp. 169–176.
- [85] S. Koos, J. Mouret, and S. Doncieux, “Automatic system identification based on coevolution of models and tests,” in *Proc. 2009 IEEE Congr. Evol. Computation*. IEEE Press, Trondheim, Norway, 2009, pp. 560–567.
- [86] M. Mirmomeni and W. Punch, “Co-evolving data driven models and test data sets with the application to forecast chaotic time series,” in *Proc. 2011 IEEE Congr. Evol. Comput.*. IEEE Press, New Orleans, LA, USA, 2011, pp. 14–20.

- [87] D. Le Ly and H. Lipson, “Optimal experiment design for coevolutionary active learning,” *IEEE Trans. Evol. Computation*, vol. 18, no. 3, pp. 394–404, 2014.
- [88] B. Kouchmeshky, W. Aquino, J. C. Bongard, and H. Lipson, “Co-evolutionary algorithm for structural damage identification using minimal physical testing,” *International Journal for Numerical Methods in Engineering*, vol. 69, no. 5, pp. 1085–1107, 2007. [Online]. Available: <http://dx.doi.org/10.1002/nme.1803>
- [89] M. Mirmomeni and W. Punch, “Co-evolving data driven models and test data sets with the application to forecast chaotic time series,” in *2011 IEEE Congress on Evolutionary Computation*. Auburn University, New Orleans, LA, 2011, pp. 14–20.
- [90] J. Bongard, V. Zykov, and H. Lipson, “Resilient machines through continuous self-modeling,” *Sci.*, vol. 314, no. 5802, pp. 1118–1121, 2006.
- [91] S. Koos, J. B. Mouret, and S. Doncieux, “The transferability approach: Crossing the reality gap in evolutionary robotics,” *IEEE Trans. Evol. Computation*, vol. 17, no. 1, pp. 122–145, Feb 2013.
- [92] A. Cully, J. Clune, D. Tarapore, and J.-B. Mouret, “Robots that can adapt like animals,” *Nature*, vol. 521, no. 7553, pp. 503–507, 2015.
- [93] P. J. O’Dowd, M. Studley, and A. F. T. Winfield, “The distributed co-evolution of an on-board simulator and controller for swarm robot behaviours,” *Evol. Intell.*, vol. 7, no. 2, pp. 95–106, 2014.
- [94] N. Jakobi, P. Husbands, and I. Harvey, “Noise and the reality gap: the use of simulation in evolutionary robotics,” in *Advances in Artificial Life: Proc. 3rd European Conf. Artificial Life*. Springer-Verlag, 1995, pp. 704–720.
- [95] B. Hedwig and J. F. A. Poulet, “Complex auditory behaviour emerges from simple reactive steering,” *Nature*, vol. 430, no. 7001, pp. 781–785, 2004.
- [96] E. Baird, M. J. Byrne, J. Smolka, E. J. Warrant, and M. Dacke, “The dung beetle dance: An orientation behaviour?” *PLoS ONE*, vol. 7, no. 1, p. e30211, 01 2012. [Online]. Available: <http://dx.doi.org/10.1371/journal.pone.0030211>
- [97] M. D. M. Byrne, “Visual cues used by ball-rolling dung beetles for orientation,” *Journal of Comparative Physiology A: Neuroethology, Sensory, Neural, and Behavioral Physiology*, vol. 189, no. 6, pp. 411–418, 2003.

Bibliography

- [98] E. G. Matthews, "Observations on the ball-rolling behavior of *canthon pilularius*," *Psyche*, pp. 75–93, 1963.
- [99] S. Garnier, J. Gautrais, and G. Theraulaz, "The biological principles of swarm intelligence," *Swarm Intelligence*, vol. 1, no. 1, pp. 3–31, 2007. [Online]. Available: <http://dx.doi.org/10.1007/s11721-007-0004-y>
- [100] C. W. Reynolds, "Flocks, herds, and schools: A distributed behavioral model," *Computer Graphics*, vol. 21, no. 4, pp. 25–34, 1987.
- [101] R. Jeanson, C. Rivault, J.-L. Deneubourg, S. Blanco, R. Fournier, C. Jost, and G. Theraulaz, "Self-organized aggregation in cockroaches," *Animal Behaviour*, vol. 69, no. 1, pp. 169 – 180, 2005. [Online]. Available: <http://www.sciencedirect.com/science/article/pii/S0003347204002428>
- [102] C. R. Carroll and D. H. Janzen, "Ecology of foraging by ants," *Annu. Review of Ecology and Systematics*, vol. 4, pp. 231–257, 1973.
- [103] J. E. Lloyd, "Bioluminescent communication in insects," *Annual Review of Entomology*, vol. 16, pp. 97–122, 1971.
- [104] O. H. Bruinsma, "An analysis of building behaviour of the termite *macrotermes subhyalinus* (rambur)," Ph.D. dissertation, Wageningen University, Wageningen, The Netherlands, 1979.
- [105] M. Dorigo and L. Gambardella, "Ant colony system: a cooperative learning approach to the traveling salesman problem," *Evolutionary Computation, IEEE Transactions on*, vol. 1, no. 1, pp. 53–66, 1997.
- [106] J. Kennedy and R. Eberhart, "Particle swarm optimization," in *Neural Networks, 1995. Proceedings., IEEE International Conference on*, vol. 4, Nov 1995, pp. 1942–1948 vol.4.
- [107] O. Holland and C. Melhuish, "Stigmergy, self-organization, and sorting in collective robotics," *Artificial Life*, vol. 5, no. 2, pp. 173–202, 1999.
- [108] G. Di Caro and M. Dorigo, "Antnet: Distributed stigmergetic control for communications networks," *J. Artif. Int. Res.*, vol. 9, no. 1, pp. 317–365, Dec. 1998. [Online]. Available: <http://dl.acm.org/citation.cfm?id=1622797.1622806>

- [109] K. Socha, “Aco for continuous and mixed-variable optimization,” in *Ant Colony Optimization and Swarm Intelligence*, ser. Lecture Notes in Computer Science, M. Dorigo, M. Birattari, C. Blum, L. Gambardella, F. Mondada, and T. Sttze, Eds. Springer Berlin Heidelberg, 2004, vol. 3172, pp. 25–36. [Online]. Available: http://dx.doi.org/10.1007/978-3-540-28646-2_3
- [110] J. Bjercknes and A. T. Winfield, “On fault tolerance and scalability of swarm robotic systems,” in *Distributed Autonomous Robotic Systems*, ser. Springer Tracts in Advanced Robotics. Springer, Berlin, Heidelberg, 2013, vol. 83, pp. 431–444.
- [111] J. Chen, M. Gauci, W. Li, A. Kolling, and R. Gros, “Occlusion-based cooperative transport with a swarm of miniature mobile robots,” *Robotics, IEEE Transactions on*, vol. 31, no. 2, pp. 307–321, April 2015.
- [112] M. Gauci, J. Chen, T. Dodd, and R. Groß, “Evolving aggregation behaviors in multi-robot systems with binary sensors,” in *Distributed Autonomous Robotic Systems*, ser. Springer Tracts in Advanced Robotics. Springer, Berlin, Heidelberg, 2014, vol. 104, pp. 355–367.
- [113] E. ahin, “Swarm robotics: From sources of inspiration to domains of application,” in *Swarm Robotics*, ser. Lecture Notes in Computer Science, E. ahin and W. Spears, Eds. Springer Berlin Heidelberg, 2005, vol. 3342, pp. 10–20. [Online]. Available: http://dx.doi.org/10.1007/978-3-540-30552-1_2
- [114] B. Gerkey and M. Mataric, “Sold!: auction methods for multirobot coordination,” *Robotics and Automation, IEEE Transactions on*, vol. 18, no. 5, pp. 758–768, Oct 2002.
- [115] A. F. T. Winfield, “Distributed sensing and data collection via broken ad hoc wireless connected networks of mobile robots,” in *Distributed Autonomous Robotic Systems 4*, L. Parker, G. Bekey, and J. Barhen, Eds. Springer Japan, 2000, pp. 273–282. [Online]. Available: http://dx.doi.org/10.1007/978-4-431-67919-6_26
- [116] V. Trianni, R. Gro, T. Labella, E. ahin, and M. Dorigo, “Evolving aggregation behaviors in a swarm of robots,” in *Advances in Artificial Life*, ser. Lecture Notes in Computer Science, W. Banzhaf, J. Ziegler, T. Christaller, P. Dittrich, and J. Kim, Eds. Springer Berlin Heidelberg, 2003, vol. 2801, pp. 865–874. [Online]. Available: http://dx.doi.org/10.1007/978-3-540-39432-7_93

- [117] S. Garnier, C. Jost, J. Gautrais, M. Asadpour, G. Caprari, R. Jeanson, A. Grimal, and G. Theraulaz, “The embodiment of cockroach aggregation behavior in a group of micro-robots,” *Artificial Life*, vol. 14, no. 4, pp. 387–408, Oct. 2008. [Online]. Available: <http://dx.doi.org/10.1162/artl.2008.14.4.14400>
- [118] A. Howard, M. J. Matarić, and G. S. Sukhatme, “Mobile sensor network deployment using potential fields: A distributed, scalable solution to the area coverage problem,” in *Distributed Autonomous Robotic Systems 5*. Springer, 2002, pp. 299–308.
- [119] J. McLurkin and J. Smith, “Distributed algorithms for dispersion in indoor environments using a swarm of autonomous mobile robots,” in *7th International Symposium on Distributed Autonomous Robotic Systems (DARS)*. Citeseer, 2004.
- [120] K. Fujibayashi, S. Murata, K. Sugawara, and M. Yamamura, “Self-organizing formation algorithm for active elements,” in *Reliable Distributed Systems, 2002. Proceedings. 21st IEEE Symposium on*, 2002, pp. 416–421.
- [121] J. Chen, M. Gauci, M. J. Price, and R. Groß, “Segregation in swarms of e-puck robots based on the brazil nut effect,” in *Proceedings of the 11th International Conference on Autonomous Agents and Multiagent Systems - Volume 1*, ser. AAMAS '12. Richland, SC: International Foundation for Autonomous Agents and Multiagent Systems, 2012, pp. 163–170. [Online]. Available: <http://dl.acm.org/citation.cfm?id=2343576.2343599>
- [122] A. Turgut, H. elikkanat, F. Gke, and E. ahin, “Self-organized flocking in mobile robot swarms,” *Swarm Intelligence*, vol. 2, no. 2-4, pp. 97–120, 2008. [Online]. Available: <http://dx.doi.org/10.1007/s11721-008-0016-2>
- [123] E. B. C.R. Kube, “Collective robotics: from social insects to robots,” *Adaptive Behavior*, vol. 2, no. 2, pp. 189–218, 1993.
- [124] C. Kube and E. Bonabeau, “Cooperative transport by ants and robots,” *Robotics and Autonomous Systems*, vol. 30, no. 12, pp. 85 – 101, 2000. [Online]. Available: <http://www.sciencedirect.com/science/article/pii/S0921889099000664>
- [125] R. Gross and M. Dorigo, “Towards group transport by swarms of robots,” *Int. J. Bio-Inspired Comput.*, vol. 1, no. 1/2, pp. 1–13, Jan. 2009. [Online]. Available: <http://dx.doi.org/10.1504/IJBIC.2009.022770>

- [126] J. Werfel, K. Petersen, and R. Nagpal, “Designing collective behavior in a termite-inspired robot construction team,” *Science*, vol. 343, no. 6172, pp. 754–758, 2014.
- [127] G. S. Fraenkel and D. L. Gunn, *The Orientation of Animals: Kineses, Taxes, and Compass Reactions*. New York: Dover Publications, 1961.
- [128] S. D. Sulkin, “Larval orientation mechanisms: The power of controlled experiments,” *Ophelia*, vol. 32, no. 1-2, pp. 49–62, 1990.
- [129] I. Rano, “A steering taxis model and the qualitative analysis of its trajectories,” *Adaptive Behaviour*, vol. 17, no. 3, pp. 197–211, 2009.
- [130] S. Camazine, *Self-organization in biological systems*. Princeton University Press, 2003.
- [131] B. Webb, “What does robotics offer animal behaviour?” *Animal Behaviour*, vol. 60, no. 5, pp. 545 – 558, 2000. [Online]. Available: <http://www.sciencedirect.com/science/article/pii/S0003347200915148>
- [132] —, “Using robots to model animals: a cricket test,” *Robotics and Autonomous Systems*, vol. 16, no. 2134, pp. 117 – 134, 1995. [Online]. Available: <http://www.sciencedirect.com/science/article/pii/0921889095000445>
- [133] A. Popov and V. Shuvalov, “Phonotactic behavior of crickets,” *J. of Comparative Physiology*, vol. 119, no. 1, pp. 111–126, 1977.
- [134] A. M. Farah and T. Duckett, “Reactive localisation of an odour source by a learning mobile robot,” in *In Proceedings of the Second Swedish Workshop on Autonomous Robotics*. SWAR Stockholm, Sweden, 2002, pp. 29–38.
- [135] A. Lilienthal and T. Duckett, “Experimental analysis of smelling braitenberg vehicles,” in *In Proceedings of the ieee international conference on advanced robotics*. Coimbra, Portugal, 2003, pp. 58–63.
- [136] T. Balch, F. Dellaert, A. Feldman, A. Guillory, C. Isbell, Z. Khan, S. Pratt, A. Stein, and H. Wilde, “How multirobot systems research will accelerate our understanding of social animal behavior,” *Proceedings of the IEEE*, vol. 94, no. 7, pp. 1445 –1463, 2006.

- [137] J. Chappell and S. Thorpe, “Ai-inspired biology: Does ai have something to contribute to biology?” *Proceedings of the International Symposium on AI Inspired Biology: A Symposium at the AISB 2010 Convention, Leicester, UK*, 2010.
- [138] J. Faria, J. Dyer, R. Clément, *et al.*, “A novel method for investigating the collective behaviour of fish: Introducing ‘robofish’,” *Behavioral Ecology and Sociobiology*, vol. 64, no. 8, pp. 1211–1218, 2010.
- [139] J. Halloy, F. Mondada, S. Kernbach, *et al.*, “Towards bio-hybrid systems made of social animals and robots,” in *Biomimetic and Biohybrid Systems*, ser. Lecture Notes in Comput. Sci. Springer, Berlin, Heidelberg, Germany, 2013, vol. 8064, pp. 384–386.
- [140] J. Halloy, G. Sempo1, G. Caprari, *et al.*, “Social integration of robots into groups of cockroaches to control self-organized choices,” *Sci.*, vol. 318, no. 5853, pp. 1155–1158, 2007.
- [141] T. Schmickl, S. Bogdan, L. Correia, *et al.*, “Assisi: Mixing animals with robots in a hybrid society,” in *Biomimetic and Biohybrid Systems*, ser. Lecture Notes in Comput. Sci. Springer, Berlin, Heidelberg, Germany, 2013, vol. 8064, pp. 441–443.
- [142] R. Vaughan, N. Sumpter, J. Henderson, *et al.*, “Experiments in automatic flock control,” *Robot. and Autonomous Syst.*, vol. 31, no. 1, pp. 109–117, 2000.
- [143] J. Krause, A. F. Winfield, and J.-L. Deneubourg, “Interactive robots in experimental biology,” *Trends in Ecology and Evolution*, vol. 26, no. 7, pp. 369 –375, 2011.
- [144] S. G. Halloy J., “Social integration of robots into groups of cockroaches to control self-organized choices,” *Science*, vol. 318, no. 5853, pp. 1155–1158, 2007. [Online]. Available: <http://www.sciencemag.org/cgi/content/abstract/sci;318/5853/1155>
- [145] J. Krause, A. F. Winfield, and J.-L. Deneubourg, “Interactive robots in experimental biology,” *Trends in Ecology and Evolution*, vol. 26, no. 7, pp. 369 –375, 2011. [Online]. Available: <http://www.sciencedirect.com/science/article/pii/S0169534711000851>
- [146] R. Vaughan, N. Sumpter, A. Frost, and S. Cameron, “Robot sheepdog project achieves automatic flock control,” *The fourth international conference*

- on *Autonomous agents*, pp. 489–493, 1998. [Online]. Available: <http://citeseerx.ist.psu.edu/viewdoc/summary?doi=10.1.1.38.3029>
- [147] A. Gribovskiy, J. Halloy, J.-L. Deneubourg, H. Bleuler, and F. Mondada, “Towards mixed societies of chickens and robots,” in *Intelligent Robots and Systems (IROS), 2010 IEEE/RSJ International Conference on*. Boston, Massachusetts: MIT press, 2010, pp. 4722–4728.
 - [148] V. Kopman, J. Laut, G. Polverino, *et al.*, “Closed-loop control of zebrafish response using a bioinspired robotic-fish in a preference test,” *J. of The Roy. Soc. Interface*, vol. 10, no. 78, pp. 1–8, 2013.
 - [149] A. M. Turing, “Computing machinery and intelligence,” *Mind*, vol. 59, no. 236, pp. 433–460, 1950.
 - [150] S. Harnad, “Minds, machines and turing: The indistinguishability of indistinguishables,” *J. Logic, Language and Inform.*, vol. 9, no. 4, pp. 425–445, 2000.
 - [151] J. L. Elman, “Finding structure in time,” *Cognitive Sci.*, vol. 14, no. 2, pp. 179–211, 1990.
 - [152] H.-G. Beyer, *The Theory of Evolution Strategies*. Berlin, Heidelberg, Germany: Springer, 2001.
 - [153] H.-G. Beyer and H.-P. Schwefel, “Evolution strategies - a comprehensive introduction,” *Natural Computing*, vol. 1, no. 1, pp. 3–52, 2002.
 - [154] A. Eiben and J. E. Smith, *Introduction to evolutionary computing*. Berlin, Heidelberg: Springer-Verlag, 2003.
 - [155] X. Yao, Y. Liu, and G. Lin, “Evolutionary programming made faster,” *IEEE Trans. on Evol. Comput.*, vol. 3, no. 2, pp. 82–102, 1999.
 - [156] F. Mondada, M. Bonani, X. Raemy, *et al.*, “The e-puck, a robot designed for education in engineering,” in *Proc. 9th Conf. on Autonomous Robot Systems and Competitions*, vol. 1. IPCB: Instituto Politécnico de Castelo Branco, 2009, pp. 59–65.
 - [157] W. Li, M. Gauci, and R. Groß, “Coevolutionary learning of swarm behaviors without metrics,” in *Proceedings of the 2014 Genetic and Evolutionary Computation Conference*. ACM Press, Vancouver, Canada, 2014, pp. 201–208.

Bibliography

- [158] S. Magnenat, M. Waibel, and A. Beyeler, “Enki: The fast 2D robot simulator,” <http://home.gna.org/enki/>, 2011.
- [159] R. L. Graham and N. J. A. Sloane, “Penny-packing and two-dimensional codes,” *Discrete and Computational Geometry*, vol. 5, no. 1, pp. 1–11, Jan. 1990.
- [160] P. Levi and S. Kernbach, *Symbiotic Multi-Robot Organisms: Reliability, Adaptability, Evolution*. Berlin, Heidelberg: Springer-Verlag, 2010.
- [161] B. Eldridge and A. Maciejewski, “Limited bandwidth recognition of collective behaviors in bio-inspired swarms,” in *Proc. 2014 Int. Conf. Autonomous Agents and Multi-Agent Syst.* IFAAMAS Press, Paris, France, 5 2014, pp. 405–412.
- [162] G. Bradski and A. Kaehler, *Learning OpenCV: Computer Vision with the OpenCV Library*. Sebastopol, CA: O’Reilly Media, 2008.
- [163] M.-K. Hu, “Visual pattern recognition by moment invariants,” *IRE Transactions on Information Theory*, vol. 8, no. 2, pp. 179–187, 1962.
- [164] W. Li, M. Gauci, J. Chen, and R. Groß, “Online supplementary material,” <http://naturalrobotics.group.shef.ac.uk/supp/2014-006/>, 2014.
- [165] R. D. King, J. Rowland, *et al.*, “The automation of science,” *Sci.*, vol. 324, no. 5923, pp. 85–89, 2009.
- [166] M. Schmidt and H. Lipson, “Distilling free-form natural laws from experimental data,” *Sci.*, vol. 324, no. 5923, pp. 81–85, 2009.
- [167] E. Martin, *Macmillan Dictionary of Life Sciences (2nd ed.)*. London: Macmillan Press, 1983.
- [168] M. Dacke, M. J. Byrne, C. H. Scholtz, and E. J. Warrant, “Lunar orientation in a beetle,” *Proc. of the Roy. Soc. of London. Series B: Biological Sci.*, vol. 271, no. 1537, pp. 361–365, 2004.
- [169] E. Baird, M. J. Byrne, J. Smolka, E. J. Warrant, and M. Dacke, “The dung beetle dance: an orientation behaviour?” *PLoS ONE*, vol. 7, no. 1, p. e30211, 2012.
- [170] H. Beyer, *The theory of evolution strategies*. Berlin: Springer, 2011.
- [171] L. Grossman, “Computer literacy tests: Are you human?” June 2008. [Online]. Available: <http://www.time.com/time/magazine/article/0,9171,1812084,00.html>